DIPARTIMENTO DI MEDICINA MOLECOLARE E DELLO SVILUPPO

DOTTORATO DI RICERCA IN MEDICINA MOLECOLARE

CICLO XXXIV

COORDINATORE PROF. VINCENZO SORRENTINO

EVALUATION OF ENDOPLASMIC RETICULUM (ER) STRESS MARKERS IN SKELETAL MUSCLE BIOPSIES FROM PATIENTS AFFECTED BY CENTRAL CORE DISEASE

SETTORE SCIENTIFICO DISCIPLINARE: BIO/17

TUTOR

Prof.ssa Daniela Rossi

DOTTORANDO

Dott.ssa Maria Rosaria Catallo

Maria Rosaria Catallo

Firmato digitalmente da Maria Rosaria Catallo
Data: 2022.06.23 19:56:02 +02'00'

Anno Accademico 2020 – 2021

INDEX

Abstract

The sarcoplasmic reticulum plays a pivotal role in regulating muscle contraction given its role in in storage, release and reuptake of Ca^{2+}. Release of calcium from the sarcoplasmic reticulum occurs through the so-called excitation-contraction coupling mechanism that consists in the activation of voltage-induced calcium channels on the plasma membrane (DHPR) with the consequent opening of ryanodine receptors type 1 (RyR1) on the sarcoplasmic reticulum. Mutations in the gene coding for RyR1 were identified in a significant fraction of human congenital myopathies, defined as RyR1-related myopathies (RyR-RM). Among these, Central Core Disease (CCD) represents the most common inherited congenital myopathy and is characterized by the presence of cores, i.e. areas lacking oxidative enzymes due to depletion of mitochondria, accompanied also by alterations in calcium homeostasis, ultrastructural modifications and induction of cellular dysfunctions such as oxidative/nitrosative stress. Recently, endoplasmic reticulum (ER) stress has been also suggested to play a relevant role in the pathophysiology of muscle disorders. ER stress is activated by a variety of conditions, including alteration in calcium homeostasis, which may lead to the accumulation of misfolded proteins and thus trigger the Unfolded Protein Response (UPR). Deregulation of ER stress/UPR is observed in many muscular diseases, including a mouse model of CCD.

In order to evaluate whether ER stress markers are also deregulated in muscles from human patients affected by CCD, expression of selected ER stress-related genes has been analyzed by real-time PCR in muscle biopsies from a cohort of twenty-two unrelated CCD patients and compared with that of healthy controls. No significant changes in expression of ER stress markers were observed in these biopsies indicating that pathogenic mechanism other than ER stress/UPR may be active in humans.

1. Introduction

1.1 Skeletal muscle: main features

Muscle tissue is an excitable tissue composed by highly specialized cells responsible for muscle contraction. Based on the different structural traits and the different role they perform, they are distinguished in cardiac, smooth and skeletal muscles (Monesi, 2012). Skeletal muscle is a striated tissue responsible for voluntary muscle contraction activated by motoneurons' stimulation. Skeletal muscle tissue is formed by multinucleated cells, called skeletal muscle fibers, which originate from the fusion of several single muscle cells that form an elongated cellular syncytium containing hundreds of nuclei, reaching a length of several centimeters with a diameter of 10-100 µm. The plasma membrane, that in muscle tissue is called sarcolemma, forms invaginations, called T-tubules, extending throughout the fibers that are responsible for the propagation of the action potential along the central part of the fibers (Jayasinghe and Launikonis, 2013). The sarcolemma surrounds the cytoplasm, also called sarcoplasm, where most of the available space is occupied by the contractile apparatus organized in myofibrils. In the sarcoplasm, the sarcoplasmic reticulum (SR) and other organelles are organized according to the organization of myofibrils, with nuclei positioned at the periphery of muscle fiber (Greising et al., 2012; Frontera and Ochala, 2015, Figure 1).

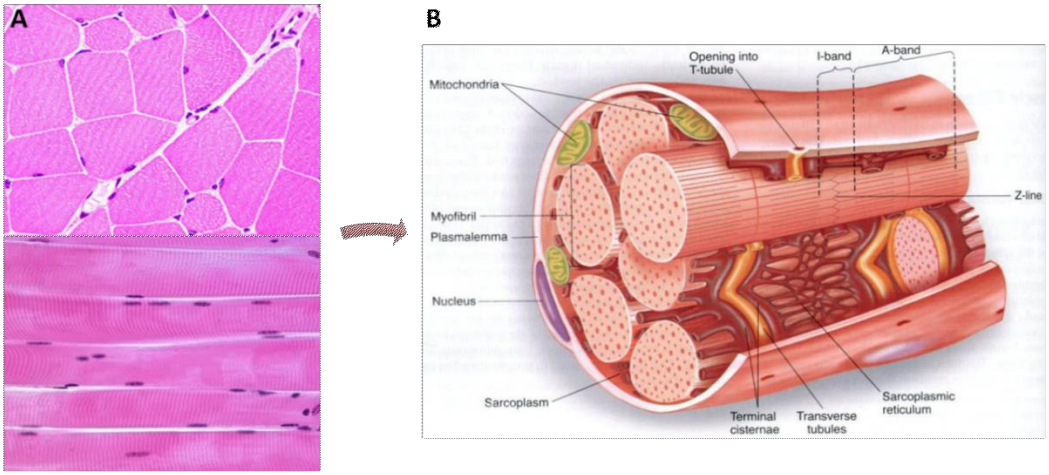

Figure 1. Skeletal muscle structure. A. *cross and longitudinal sections of human skeletal muscle, stained with Hematoxilin – Eosin.* ***B.*** *Schematic representation of skeletal muscle structure. (Image adapted from http://medcell.med.yale.edu; https://www.brianmac.co.uk).*

1.1.1 Myofibrils

The well-defined arrangement of myofibrils, placed parallel and aligned along the longitudinal axis of the muscle fiber, gives the fiber its typical cross-banding aspect. A single myofibril is 1-3 µm thick, composed by regular repeating units called sarcomeres of approximately 2.2 µm in length, which represent the functional contractile units of skeletal muscle. Polarized light microscopy makes fibers look striated with less dense isotropic bands, called I bands and dark anisotropic bands, called A bands. At the electron microscope also the H bands and the M bands, placed at the center of the A band, are detected. Lastly, the I band is divided in half by the Z disk. Each segment of a myofibril between two consecutive Z disks correspond to one sarcomere. Under the electron microscope, the sarcomere appears cross-banded because of the presence of two types of filaments, commonly known as the thick and thin myofilaments, which differ in dimension and protein content. The thick myofilaments are mainly composed by myosin, while the thin myofilaments are mainly composed by actin (Figure 2). The interaction between actin and myosin filaments is possible thank to two regulatory proteins: tropomyosin and troponin, which regulate the exposure of the myosin binding site on actin, under Ca^{2+} dependent mechanism, during muscle contraction (Monesi, 2012).

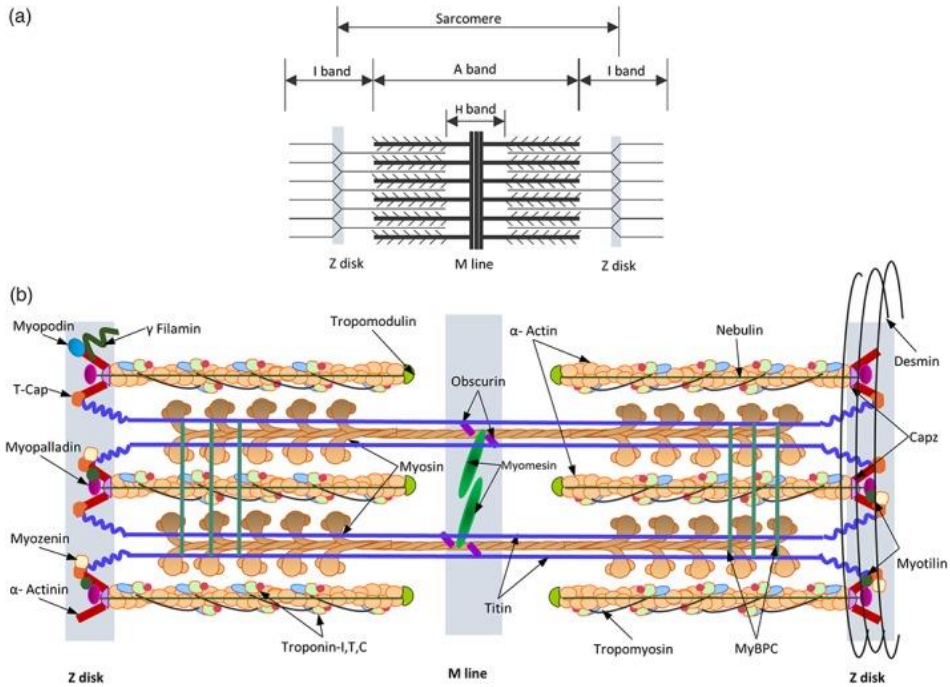

Figure 2. Sarcomere representation: *schematic representation of a segment of a muscle fiber and the composition of a myofibril: parallel and regular disposition of thick and thin filaments give the myofibrils its striated aspect (Mukund et al, 2020).*

1.1.2 Sarcoplasmic/endoplasmic reticulum in skeletal muscle

The sarcoplasmic reticulum is a specialized form of endoplasmic reticulum (ER) dedicated to storage and release of Ca^{2+} following sarcolemma depolarization, to activate muscle contraction. It develops during embryonic life starting from an accumulation of membranes, which, in post-natal life, evolve in two different, but functionally linked domains: junctional sarcoplasmic reticulum (j-SR) and longitudinal sarcoplasmic reticulum (l-SR). The l-SR is composed by a network of tubules that surround each myofibril, placed parallel, and usually longitudinally oriented. l-SR is the main site for Ca^{2+} storage and uptake from the cytosol, a process depending on the SR/ER Ca^{2+}-ATPase (SERCA) pumps (Bublitz et al., 2013). The longitudinal tubules at their far end form the so-called terminal cisternae, which constitute the j-SR, oriented in a transversal direction. Two terminal cisternae are regularly placed on the opposite sides of a central T-tubule, an invagination of the sarcolemma, forming a structure known as junctional triad, directly involved in Ca^{2+} release (Franzini-Armstrong, 1970; Treves et al., 2017).

Although ER-related functions (such as Ca^{2+} storage, protein synthesis and folding and lipid sterol synthesis) are undoubtedly present in striated muscle cells, the distribution of the ER within the SR membranes is less obvious (Rossi et al, 2022). It is accepted that the SR and ER form a continuous membrane system composed of different specialized subdomains (Volpe et al, 1992). By means of localization of ER and SR markers in skeletal muscle fibres, a certain compartmentalization has been demonstrated: ER-specific proteins were detected at the perinuclear region and in two distinct rough ER sub-compartments, respectively located in correspondence of the I band, which doesn't contain ER exit sites, and close to the Z disk, which shows export activity towards the Golgi (Rossi et al, 2008; Kaisto and Metsikkö, 2003). Interactions existing between ER and other intracellular components in skeletal muscle are still under investigation. Lysosome-SR junctions have been observed in pulmonary arterial myocytes. These nanojunctions have been detected between clusters of lysosomes and perinuclear regions of the SR rich in RyR3 and may represent an intracellular structure involved in the regulation of specific Ca^{2+} signaling events (Kinnear et al, 2008). Studies rabbit ventricular myocytes have also revealed the presence of SE-lysosome contact sites, that, unlike what previously described in pulmonary arterial myocytes, are distributed with a frequency compatible with the length of a sarcomere, allowing the association with specific areas of the SR with lyososomes (Aston et al, 2017; Rossi et al, 2022).

1.1.3 The junctional triad

The junctional triad represents the site of physical interaction between the voltage gated L-type calcium channel dihydropiridine receptor (DHPR), located on the T-tubules, and the ryanodine receptor Ca^{2+} release channel type 1 (RyR1); on this interaction depends the depolarization-induced calcium release (DICR) mechanism that, following depolarization of T-tubules, allows calcium ions to be released from the SR to the cytosol and myofilaments to contract (Rios, 2018; Barone et al., 2015). The so-called excitation-contraction coupling (E-C coupling) is a sequence of events that, starting from depolarization of the sarcolemma induced by a motoneuron leads to muscle contraction (Sandow, 1965). The first event of E-C coupling is the release of acetylcholine from a pre-synaptic element. Acetylcholine interacts with its receptor, localized on the sarcolemma, causing Na^{+}-dependent depolarization (Takamori, 2012). Depolarization is passively conducted down to the T-tubules where it activates the DHPR channels. During depolarization of the T-tubule DHPR channels undergo a conformational change; since DHPR and RyR1 are physically in contact, the conformational change in DHPR is immediately transmitted to RyR1, resulting in channel opening and Ca^{2+} release from the terminal cisternae (Greising et al., 2012). At the end of a nervous stimulus, Ca^{2+} is re-uptaken by SERCA pumps and stored in the SR, while the plasma membrane Ca^{2+}-ATPase (PMCA) pumps Ca^{2+} from the cytoplasm to the extracellular environment, together with the Na^{+}/ Ca^{2+}-exchanger (NCX), thus allowing Ca^{2+} to return to basal levels (Sandor, 1965; Brini et al., 2013) (Figure 3).

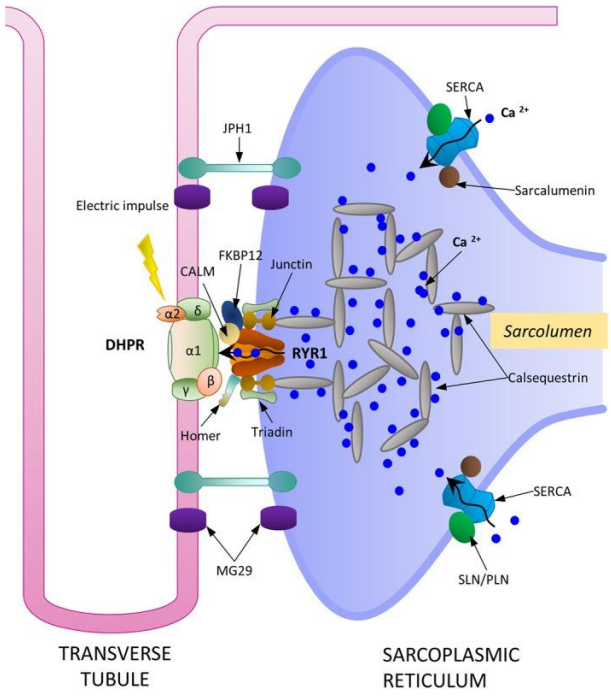

***Figure 3**. **Triad**. A schematic representation of the main molecular actors involved in excitation contraction coupling at the triad junction. DHPR, RYR1, SERCA pump, along with calsequestrin form the main proteins responsible for Ca^{2+} cycling and storage within the sarcoplasmic reticulum. (Mukund et al, 2020)*

1.1.4 Ryanodine Receptors, RYRs

RyRs are intracellular calcium release channels that facilitate the rapid release of Ca^{2+} from stores in the SR into the cytosol (Zalk et al. 2015). There are three RyR genes in a mammalian genome (*RYR1, RYR2 and RYR3*) coding for three distinct proteins that share about 66% of their amino acid sequence. The homology among the three isoforms is not equally distributed, with some regions sharing more than 90% of homology and three specific regions where the homology is significantly lower. These three regions have been named divergent regions, D1–D3. Within RyR1 sequence, region D1 spans amino acids 4254–4631, region D2 amino acids 1342–1403 and region D3 lies between residues 1872 and 1923. These regions are expected to correspond to isoform-specific regulatory sites with specific properties of these channels (Sorrentino et al, 2000). RYR1 and RYR2 have an 80 % amino acid sequence similarity, but functionally they work in a different manner: in contrast to the mechanical activation of RYR1, RYR2 opening is triggered by the influx of extracellular Ca^{2+} across the cardiac voltage gated Ca^{2+} channels (Cav1.2) in a process known as Ca^{2+} induced Ca^{2+} release (CICR) (Saito et al, 1988).

1.2 The structure of Ryanodine Receptor type 1

RyR1 is a ~2.2 MDa homotetrameric channel composed of four polypeptides each consisting of approximately 5000 amino acids with a molecular weight of ~565 kilodalton (kDa) (Yan et al., 2015; Zalk et al., 2015). Recent advances in cryogenic electron microscopy (cryo-EM) allowed several structures of the RyR1 channel to be elucidated at 3.8-4.8 Armstrong (A) resolution (Yan et al., 2015; Zalk et al., 2015; des Georges et al., 2016). RyRs have a typical mushroom appearance, with the stalk crossing the ER/SR membrane and the cap, representing about 80% of the entire protein, that protrudes completely in the cytosol. The cytosolic cap mediates ligand-sensing in the channel as well as providing a scaffold for modulatory interactions with a number of intracellular proteins, including Cav1.1 and small molecules (Yan et al, 2015; Zalk et al, 2015; des Georges et al, 2016). The latter include caffeine, halothane, Ca^{2+}, Mg^{2+}, adenosine triphosphate (ATP) (Amador et al, 2013). The transmembrane (TM) domain is composed by six transmembrane helices and forms the pore for Ca^{2+} movement out of the SR. Each one of the cytosolic monomers of the tetramer is built around an extended scaffold of alpha-solenoid repeats. The alpha solenoid scaffold is formed by three segments, and it is capped, at the amino terminus, by two distinct N-terminal domains (NTD-A and NTD-B); these are immediately followed by the first segment, the N-solenoid (NTD-C), which is in connection with three SPRY (SPIA kinase and ryanodine receptor) domains, surrounded by two pairs of RyR repeats (RY1&2 and RY3&4). The second and the largest alpha solenoid is represented by the bridging solenoid (B-sol), which is in connection with the third and last segment, the core-solenoid (C-Sol) (Zalk et al., 2015). The high flexibility of the alpha solenoid scaffold of RyR1 facilitates the interaction of the channel with all the regulatory proteins, thus allowing coupling of conformational changes within the scaffold, induced by protein binding (Zalk et al, 2015; des Georges et al, 2016; Hernández-Ochoa et al., 2015; Yan et al., 2015; Zalk et al., 2015; des Georges et al., 2016; Amador et al., 2013). The TM pore presents a fold shape as others six-transmembrane (6TM) superfamily ion channels (voltage-gated sodium and potassium channels and transient receptor potential (TRP) channels) (Zalk et al, 2015). This TM region contains two domains: the pore domain, formed by S5, S6, the pore helix and the P-segment and a pseudo voltage-sensor domain (pVSD), formed by S1–S4 that interfaces with the pore domain of the adjacent subunit. The S6 helix extends into the cytosol, terminating in the C-terminal domain (CTD), a small alpha-helical domain that extends laterally from the channel axis into the core solenoid, thus connecting the TM domain to

the cytosolic scaffold of RyR1 (Zalk et al, 2015). The CTD connection to the central domain is thought to act as a central transmitter of conformational changes from the ligand binding cytosolic portion to the channel forming components (Yan et al, 2015). The central domain also comprises EF hand motifs that may confer the Ca^{2+}-sensing ability to RyR1 (Yan et al., 2015; Samso 2016). The regulation of the channel activity also depends on intramolecular signal transduction mechanisms: studies with peptide probes have shown that interaction among different regions in RyRs may be responsible for channel regulation (Yamamoto et al, 2000). Interestingly, a mutation found in MH/CCD patients (Arg2458Cys) is located in one of the interaction points between the different regions, suggesting that this amino acid may have a role in interdomain interactions (Yamamoto et al, 2002).

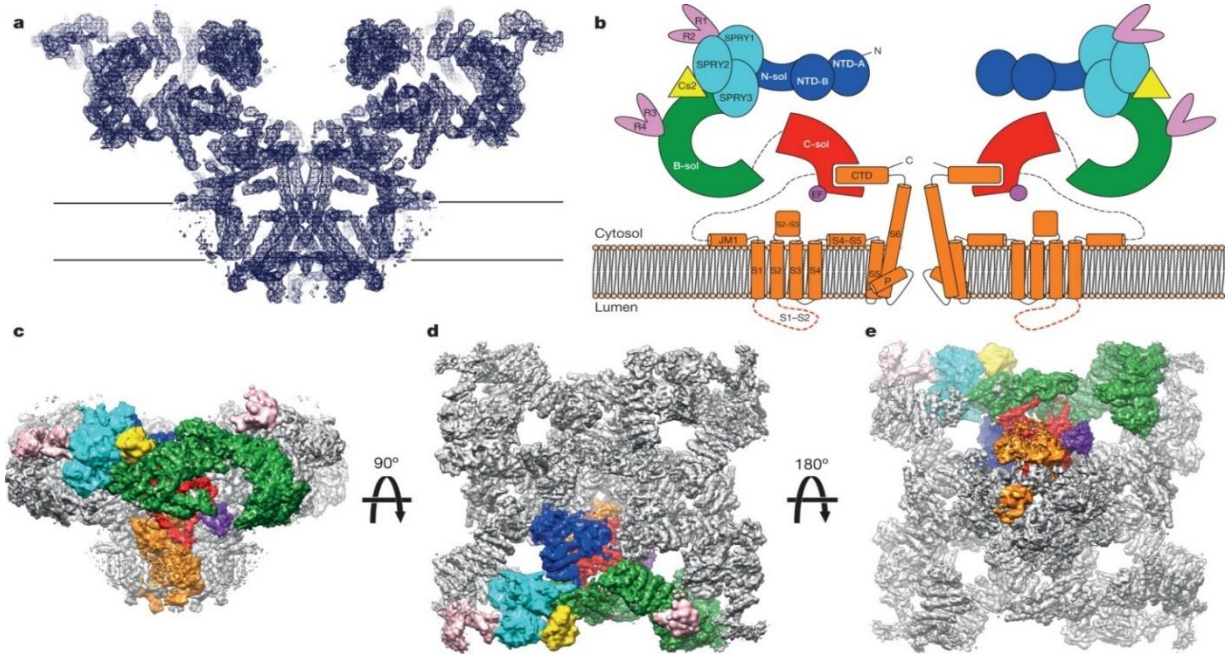

Figure 4. Representation of RyR1. ***A.*** *View from the plane of the sarcoplasmic reticulum membrane of a slab of density (blue mesh) coinciding with the channel axis.* ***B****. Schematic representation of the RyR1. B-sol, bridge solenoid; C-sol, core solenoid; N-sol, N-terminus solenoid.* ***C****. View in the plane of the sarcoplasmic reticulum membrane.* ***D.*** *View from the cytosol.* ***E****. View from the lumen of the density map of skeletal muscle RyR1 at 5.0 Å resolution, with one protomer segmented according to the domains assigned in the model, coloured as follows: blue, N-terminal domain; cyan, SPRY1, SPRY2 and SPRY3; salmon, clamp region (RY12 repeats), and phosphorylation domain (RY34 repeats); yellow, calstabin; green, the bridge solenoid scaffold; red, the core solenoid; and orange, transmembrane and C-terminal domains; purple, putative Ca^{2+}-binding domain (EF). (Zalk et al., 2015)*

1.3 RyR1 interactors and modulators

Opening RyRs is regulated by conformational changes that are induced by binding of small molecules and ions and proteins such as FKBP12, triadin, junctin and calsequestrin.

1.3.1 DHPR

Interaction between DHPRs and RyR1 is fundamental for the E-C coupling. DHPRs are multimeric complexes composed by a pore forming α1s subunit (also called Cav 1.1) (176 kDa), and auxiliary subunits α2δ (177 kDa), β (56 kDa), and γ (34 kDa) that are implicated in modulating the membrane trafficking, current kinetics, and gating properties of the channel (Samso et al., 2015; Wu et al., 2015; Zhao et al, 2019). The α1s subunit comprises four domains (I-IV) each containing 6 transmembrane alpha helical segments (S1-S6) (Hu et al., 2015). Like RyR1, Cav1.1 has structural homology with other voltage gated ion channels and S1-S4 helixes are thought to be the voltage sensing domains (VSDs). S5, S6 and the intervening segments are combined to form the ion-conduction pore domain (Bannister and Beam, 2013; Wu et al., 2015). The cytosolic β subunits are involved in tetrads assembly, where one DHPR tetrad faces one of the four subunits of the tetrameric RyR1 channel. The γ subunit is a transmembrane protein whereas the α2δ subunit is extracellular; the first one was found to interact with the VSD and the second with the extended extracellular loops of Cav1.1 (Wu et al., 2016). Loop II-III (residues 720-765) of the α1s subunit are generally accepted to interact with RyR1 and to be critical for excitation-contraction coupling (Tanabe et al, 1990). The site of interaction in RyR1 is not completely defined, since more than one region was described to be important for excitation-contraction coupling; for example, deletion of the D2 region in RyR1 (namely aa 1303–1356) abolished excitation–contraction coupling (Yamazawa et al, 1997) but also region from amino acids 1635 to 2636 was found to be relevant for channel interaction and activation (Nakai et al., 1998). From a functional point of view, it is known that, in addition to RyR1 channel opening induced by DHPR (a mechanism known as orthograde signaling), also a retrograde signaling from RyR1 to DHPR occurs in skeletal muscle. More specifically, following the initial conformational change induced by DHPR, RyR1 can transmit a retrograde signal to DHPR that enhances the inward Ca^{2+} current through the Cav 1.1 subunit (Nakai et al, 1996). A region from amino acids 1635 to 2636 of RyR1 has been found to be responsible for both orthograde and

retrograde signaling, while amino acid residues from 2659 to 3720 of RyR1 are only responsible for retrograde signaling (Nakai et al, 1998).

In the last decade, a third component of the excitation contraction coupling mechanism has been discovered. This is the Src homology 3 and cysteine rich domain 3 (STAC3) protein, which has been recognized to be involved in both trafficking of Cav 1.1 to the plasma membrane and stabilizing the DHPR-RyR1 interaction (Nelson et al, 2013; Polster et al., 2015 & 2016; Linsley et al, 2017). Recent findings suggested that the interaction between STAC3 and Cav 1.1 occurs via the SH3 domain on the former and the II-III linker in the latter (Polster et al., 2018). A variant in STAC3 was shown to be pathogenic for Native American myopathy (NAM) (Horstick et al., 2013), an autosomal recessive disorder characterized by congenital muscle weakness, delayed motor development, distinctive facies abnormalities and susceptibility to Malignant Hyperthermia (Bailey and Bloch, 1987; Horstick et al., 2013).

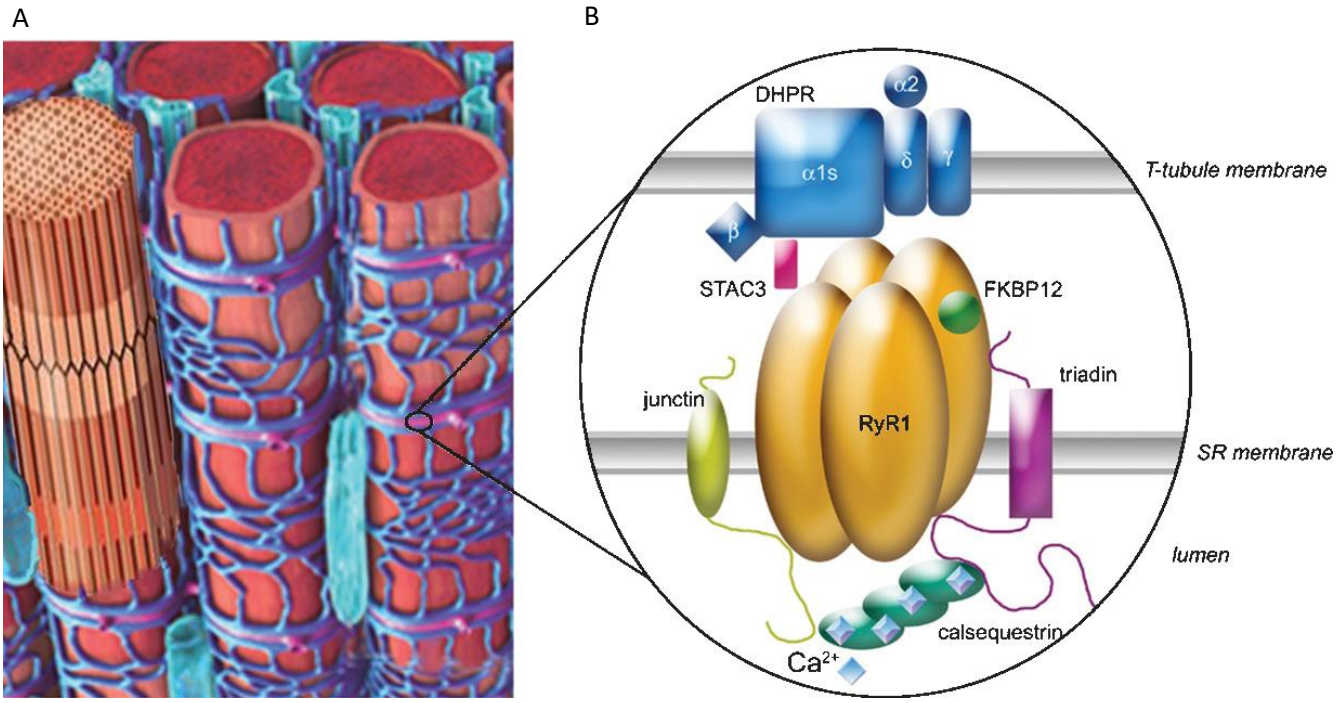

Figure 5. RyR1-DHPR interaction. A. *Representation of the site where excitation–contraction coupling occurs, at the triads of skeletal muscle, which are localized regularly at the interface between A and I bands.* ***B.*** *Schematic representation of the two calcium channels, the DHPR and RyR1, anchored in two membranes (T-tubule and sarcoplasmic reticulum (SR), respectively) and the numerous associated proteins, among which triadin, junctin, calsequestrin, FKBP12 and STAC3 (Marty et al, 2016).*

1.3.2 FKBP12

FK506-binding protein 12 (also known as FKBP12) is encoded by the *calstabin-1* gene and is located in the sarcoplasm of skeletal muscle. Four FKBP12 subunits bind to the homotetrameric RyR1 protein in a 1:1 manner (Jayaraman et al, 1992; Qi et al, 1998; Wehrens et al, 2005): it is reported that FKBPs provide a stabilizing effect on RyR channel function by lowering open probability and preventing sub-conductance state gating (Venturi et al, 2014). A second isoform of FKBP12, the FKBP12.6 protein, has been found to bind to RyR2 (Timerman et al, 1994), while RyR3 associates with both FKBP12 and FKBP12.6 (Bultynck et al, 2001). FKBP12 was also shown to support the functional interaction between DHPR and RyR1 by potentiating the open state of the RyR1 when bound to the II-III loop region of DHPR (O'Reilly et al, 2002). Interaction with FKBP12 has been proposed to be regulated by the phosphorylation of RyR1 at S2843 by PKA (Reiken et al, 2003), although this point is still controversial; PKA-dependent phosphorylation prevents the binding of Mg^{2+} and of FKBP12 to RyR1 channel thereby increasing RyR1 open probability (Reiken et al., 2003; Ruehr et al, 2003). Accordingly, dephosphorylation of RyR1 by Protein Phosphatase type 1 restores channel binding to FKBP12 (Reiken et al, 2003) and activation of the phosphodiesterase PDE4D3 reduces the effect of PKA stimulation (Bellinger et al, 2008).

1.3.3 Triadin

Triadin is a junctional SR membrane glycoprotein interacting with RyR1 both in the sarcoplasm and in the SR lumen (Groh et al, 1999; Goonasekera et al, 2007). Disruption of sarcoplasmic RyR1 and triadin interaction results in RyR1 channel inhibition; similarly, deletion of the luminal binding site for RyR2 corresponding to residues 200–224 in cardiac triadin, prevents activation of the channel (Terentyev et al, 2005) suggesting that triadin may act as a channel activator. However, other studies pointed to triadin as a negative regulator of RyR1 (Ohkura et al, 1998; Groh et al, 1999). Indeed, triadin knockout mice show no significant alteration in E-C coupling, although they show variable changes in myoplasmic and SR Ca^{2+} levels, a reduction in muscle strength and alterations in triad architecture (Eltit et al, 2010; Eltit et al, 2011; Oddoux et al, 2009; Shen et al, 2007). Triadin also interacts with calsequestrin (CSQ) in the SR lumen in a Ca^{2+} dependent manner and it has been proposed that triadin helps in anchoring CSQ in close proximity of RyR (Rossi et al, 2009). It has been also shown that CSQ itself plays a role in

triadin positioning at the j-SR since CSQ depletion results in decreased association of triadin to the j-SR (Paolini et al, 2007; Rossi et al, 2014).

1.3.4 Junctin

Juctin, like triadin is a transmembrane protein that binds CSQ and RyR1 at the j-SR; like triadin, junctin can bind RyR channels both in the cytoplasm and in the SR lumen (Li et al, 2015; Rossi et al., 2022). The luminal domain of Junctin also binds CSQ, with a functional role similar to that of triadin; nevertheless, the disruption of Triadin-CASQ interaction seems to have a more profound effect on jSR architecture and myoplasmic Ca^{2+} regulation than that of Junctin-CASQ association (Boncompagni et al, 2012). Junctin overexpression in cardiomyocites resulted in a decrease in Ca^{2+} release amplitude and contractility (Gergs et al., 2007). On the contrary, junctin knockout mice exhibited increased contractile and Ca^{2+}-cycling parameters in cardiac muscle (Yuan et al., 2007) although no significant changes in Ca^{2+} signaling were observed in skeletal muscle (Boncompagni et al., 2012), indicating that the regulatory role of junctin on RyR channels and Ca^{2+} release may be different in cardiac and skeletal muscles.

1.3.5 Calsequestrin

Calsequestrin (CSQ) is a Ca^{2+} storage glycoprotein located in the lumen of the SR where it functions as the main Ca^{2+} buffer of the SR (Szegedi et al, 1999; Shin et al, 2003). In skeletal muscles, two CSQ isoforms, CSQ1 and CSQ2 are expressed. CSQ has been shown to have an inhibitory effect on RyR1; depletion of CSQ in lipid bilayer experiments causes a 10-fold increase in calcium release, which is restored when CSQ is reintroduced in the luminal side of the channel (Beard et al, 2002). CSQ interaction with RyR1 is mediated by triadin and junctin; this correlation seems to depend on SR luminal calcium concentration as well as by phosphorylation/dephosphorylation mechanisms. Binding of CSQ to junctin and triadin is promoted when luminal Ca^{2+} is low, resulting in RyR1 inhibition. Interestingly, closure of RyRs at low Ca^{2+} concentration has been suggested to prevent dangerous SR exhaustion (Canato et al., 2010; Sztretye et al., 2011; Zima et al., 2010; Manno et al., 2017). When phosphorylated, CSQ binds to junctin only, still maintaining the closed state of RyR1, while in its dephosphorylated state, it preferentially binds triadin resulting in RyR1 activation (Beard et al, 2008; Beard et al, 2009).

1.3.6 Other RyR1 regulators

Different ligands including calcium, magnesium and adenosine triphosphate were shown to regulate RyR1 activity (MacIntosh et al, 2012; Laver et al, 2007; MacIntosh et al, 2012) (Figure 6). Single-channel recordings of RyR1 revealed that the probability plot of channel opening versus Ca^{2+} concentration is bell-shaped (Bezprozvanny, 1991). Specifically, when the Ca^{2+} concentration is lower than the nano-molar level, RyR1 is in a resting, closed state. When the Ca^{2+} concentration is between the nano-molar to micromolar level, RyR1 begins to be activated, and its opening probability reaches its maximum at 10∼100 µM Ca^{2+}. With a Ca^{2+} concentration higher than 100 µM, RyR1 begins to be inactivated and completely closes at Ca^{2+} concentrations ≥1 mM (Wei et al, 2016). The cytosolic calcium binding site in RyR1 is located in the C-terminal region close to ATP and caffeine binding sites. A luminal binding site has been proposed to include amino acid 4872 of RyR1, since mutation of this residue from Glutamic acid to alanine abolished a mechanism described as store overload-induced calcium release (SOICR); according to this mechanism an increase in the luminal calcium concentration was found to trigger or increase RyR1 opening.

ATP has an activating effect on RyR1 at its ATP-binding sites; the interaction between ATP and RyR1 is affected by Ca^{2+}, Mg^{2+} and pharmacological agents including dantrolene (Dias et al, 2009). The ATP binding site of RyR1 is located at the junction of the cytoplasmic extension of S6 (S6c) transmembrane helix and the CTD (des Georges et al, 2016).

In contrast to ATP, Mg^{2+} inhibits RyR1 activity. Mg^{2+} binds to both high affinity Ca^{2+} activation sites and Mg^{2+} inhibitory sites. When bound to the activation sites, Mg^{2+} produces an inhibitory effect by reducing RyR1 sensitivity to Ca^{2+}. Under normal physiological conditions, Mg^{2+} is bound to the RyR1 inhibitory sites, thus inhibiting the activation effect of both Ca^{2+} and ATP (Endo et al, 2009; MacIntosh et al, 2012; Copello et al, 2002).

Calmodulin (CaM) is a Ca^{2+} binding protein containing four EF-hand type Ca^{2+} binding motifs, in the N- and C-terminal regions. At nanomolar Ca^{2+} concentrations, CaM enhances RyR1 activity, while at micromolar Ca^{2+} concentrations, it inhibits the channel (Rodney et al, 2001). Moreover, CaM exists in two forms: without Ca^{2+} (apocalmodulin, apoCaM) and Ca^{2+} bound (Ca^{2+}-CaM); both can bind to RyR1, with the latter having a higher affinity (Zhang et al, 2003). ApoCaM functions as an agonist causing the

release of Ca^{2+} at low sarcoplasmic Ca^{2+} concentrations, whereas Ca^{2+}-CaM maintains the closes state of RyR1 at high sarcoplasmic Ca^{2+} concentration (Gehlert et al, 2015; Huang et al, 2012).

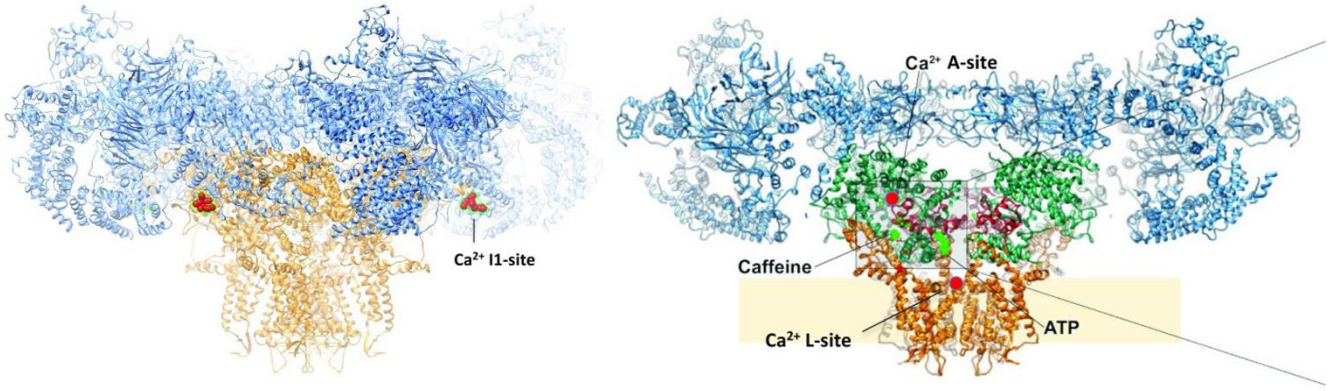

***Figure 6**. **RyR1 structure** reconstructed from cryo-EM images showing putative locations of key regulation sites on the RyR. Ca^{2+} binding sites are marked in red. Left—a distinctive sequence of 30 negative amino acids at positions 1873–1903 postulated to form the Ca^{2+}/Mg^{2+} inhibitory; I1-site (Laver et al. 1997) is shown on two of the four subunits. Right—a cutaway of the RyR1 structure showing activation sites for Ca2+ (A-site), caffeine and ATP (des Georges et al. 2016)*

1.4 RyR1 related myopathies (RyR1-RM)

Mutations in RYR1 are the most common cause of congenital myopathies (Amburgey et al, 2011). Both dominant and recessive mutations have been reported in *RYR1*. Dominant mutations have traditionally been associated with central core disease (CCD) and/or with susceptibility to malignant hyperthermia (MH), a pharmacogenetic disorder triggered by volatile anesthetics (Robinson et al, 2006). Recessive mutations predominate in patients with multiminicore disease (MmD), centronuclear myopathy (CNM), and congenital fiber type disproportion (CFTD) (Jungbluth, 2007; Clarke et al, 2010). At this time, no specific treatments are available for any RYR1-related myopathy.

1.4.1 Malignant hyperthermia

Malignant hyperthermia is a potentially lethal pharmacogenetic disorder which manifests in genetically predisposed individuals when exposed to trigger agents such as common volatile anesthetics (halothane, enflurane, isoflurane, desflurane, sevoflurane) or depolarizing neuromuscular relaxants (e.g., succinylcholine). Susceptible individuals are apparently normal and do not show signs of myopathy in their life. The exposure to triggering agents results in a hypermetabolic state, with elevated

muscle contraction. If not rapidly treated, a MH reaction has a mortality rate of 80% (Tong et al, 1997; Hopkins et al, 2015). The occurrence of MH is estimated to range from 1:5.000 to 1:50.000/100.000. Over the years, the mortality has been reduced from 80% to less than 5% by introduction of dantrolene as a specific drug for MH treatment (Rosenberg et al, 2007). MH-like crisis may also rarely develop because of exposure to other triggering agents, such as administration of drugs (neuroleptics, ecstasy), stress or vigorous exercise (Stowell et al, 2008). When exposed to triggering substances or conditions, MH susceptible individuals respond with a dysregulated and uncontrolled calcium release from the SR to the myoplasm; the resulting hypercalcemia causes hypermetabolism and early signs of the crisis such as: end-tidal CO_2 increase, skeletal muscle rigidity, cyanosis, lactic acidosis, rising blood pressure, tachycardia, hyperventilation and fever. The body temperature could rise very rapidly (1-2°C every 5 minutes). If diagnosed late, MH progresses to a multiorgan system failure that includes cardiac dysrhythmias (cardiac arrest), renal failure, and disseminated intravascular coagulation (DIC). MH is currently diagnosed by the use of the In Vitro Contracture Test, that can be performed according to the guideline introduced by European Malignant Hyperthermia Group (EMHG), with a sensitivity of 99% and a specificity of 94% or by the Malignant Hyperthermia Association of the United States (MHAUS), that define the Caffeine Halothane Contracture Test (CHCT), with a sensitivity of 97% and a specificity of 80%. Patients with a positive contracture test should also undergo genetic testing for identification of causative MH mutations. More than 200 mutations have been detected in RyR1. However, not all mutations have been functionally characterized and, at the current time, only 48 mutations in *RYR1* are considered diagnostic mutations, because well characterized by functional and genetic studies (EMHG website; Weiss et al, 2004; Eltit et al, 2012). Pathogenic MH mutations are basically gain-of-function mutations that result in hypersensitive channels (Eltit et al., 2010; Wehner et al., 2002; Ducreux et al., 2004; Yang et al., 2007). In addition to RyR1, mutations in *CACNA1S* coding for the alpha 1S subunit of DHPR have been also linked to MH. About 30% of patients positive at the IVCT do not carry mutations in either *RyR1* or *DHPR* (Miller et al., 2018).

1.4.2 Central Core Disease

Central core disease (CCD) is an inherited neuromuscular disorder defined by areas with reduced oxidative activity running along the longitudinal axis of the muscle fiber ("central cores") and clinical features of a congenital myopathy; the absence of oxidative enzyme activity in the core area is due to mitochondrial depletion (Dubowitz et al, 2020) (Figure 7). Typically, CCDs show abundant type 1 fiber predominance with only a few (or even none) type 2 fibers (Jungbluth et al, 2011). Even though not useful for diagnostic purpose, recently it has been noticed that dominantly inherited cases show “structured” cores, characterized by a striated myofibrillar pattern and myofibrillar ATPase activity; in contrast, “unstructured” cores, typical of recessive forms, are defined by a decrease in myofibrillar ATPase activity (Dubowitz et al, 2020). Proteins such as desmin, αβ-crystallin, filamin C, small heat-shock proteins, myotilin, RyR1, triadin, and DHPR accumulate in the cores (Ogasawara, 2021). Patients diagnosed with CCD show non-progressive or slowly progressive weakness in truncal and proximal muscles; patients often show orthopedic difficulties such as congenital hip dislocation, scoliosis, and clubfoot deformities (Manzur et al, 1998). Depending on the severity of the mutation, the wide range of manifestation could include severe muscle weakness from infancy or development of mild symptoms in late adulthood; however, even patients of the same family sharing the same *RYR1* mutation could develop a wide range of phenotype, suggesting the presence of additional risk factors (Jungbluth et al, 2011). Generally, patients with recessive *RYR1* mutations develop more severe phenotypes than those with dominant *RYR1* mutations, which may include additional signs like extraocular and bulbar muscle involvement, while more severe cases may result in fetal akinesia (Klein et al, 2012). CCD is due to *RYR1* mutations in more than 90% of patients: it is mainly caused by heterozygous missense mutations affecting the C-terminal pore forming domain of RyR1 (Wu et al, 2006). Dominant forms of CCD are allelic to MH (Kraeva et al, 2015). Variations in the MYH7 gene are increasingly associated with CCD, covering up to 10% of CCD cases. Other genes implicated in CCD are *SEPN1*, *ACTA1*, *TTN* and *CACNA1S* (North et al, 2014; Schartner et al, 2017).

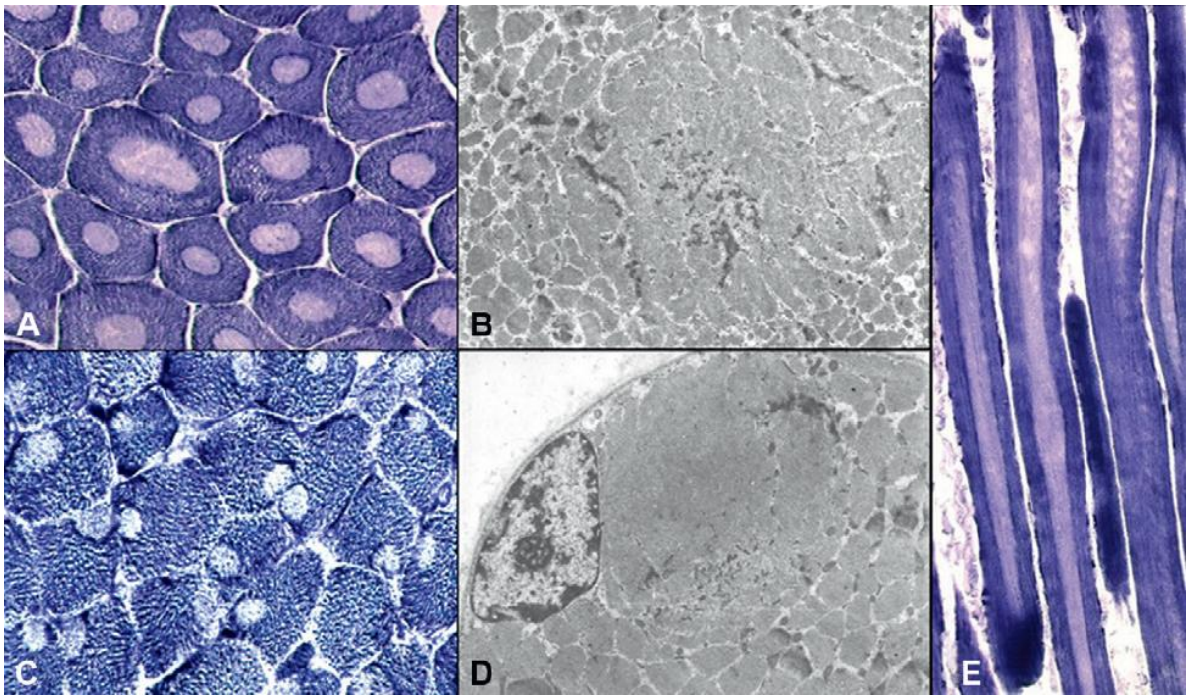

Figure 7. Central core disease. *In transverse muscle sections, the cores appear as central (**A**) or eccentric (**C**) areas of muscle fibers devoid of oxidative enzyme activity – nicotinamide adenine dinucleotide-tetrazolium reductase (NADH-TR). On electron microscopy, cores appear as disorganized sarcomeric areas with decreased numbers of mitochondria and reduced amount of glycogen (**B**, central core; **D**, eccentric core). In longitudinal section, the cores extend almost along the full length of the fibers (**E**, NADH-TR) (Romero and Clarke, 2013)*

1.4.3 Multiminicore disease

Multiminicore disease (MmD) is a recessive RYR1-RM subtype presenting numerous cores, visible as pale spots on oxidative stained muscle sections and gathered in a limited area on longitudinal section. Multiple internally located nuclei and type 1 fiber predominance are noted in affected muscle (Figure 8). Clinical features of MmD are more variable and, in addition to *RYR1*, mutations in other genes have been associated with MmD. Selenoprotein-1 (*SEPN1*)-related forms of MmD are characterized by delayed development, marked weakness, and wasting, early spinal rigidity, hip gridle involvement, scoliosis and respiratory involvement (Jungbluth et al, 2005). *RYR1*-related forms of MmD show the same clinical pattern of the *SEPN1* related type but have additional extraocular muscle involvement and a more severe respiratory impairment (Klein et al, 2012). Patients with *TTN* and *MYH7* mutations are most likely to show cardiomyopathy. Other genes that could be involved in the onset of MmD are *MEGF10* and *CACNA1S* (Schartner et al, 2017; Boyden et al, 2012).

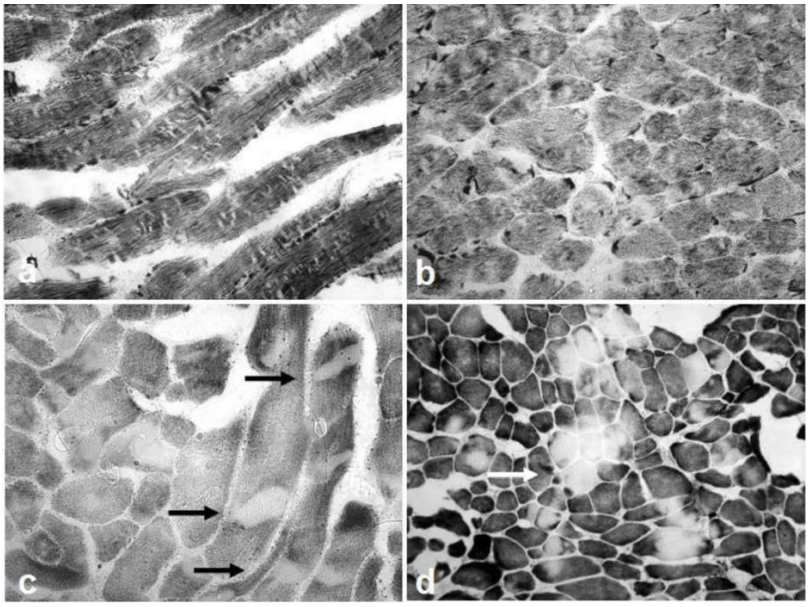

Figure 8. Histopathological features of Multi-minicore disease*. NADH-TR (**a–c**) and cytochrome oxidase (COX) (**d**) stains, longitudinal (**a,c**) and transverse (**b,d**) sections from two different samples. Predominance of darker staining type 1 fibers is prominent in both samples, whilst appearance of core lesions is widely variable, ranging from numerous small lesions of limited extent ("minicores") (**a-b**) to few multiple large lesions often extending throughout the entire fiber diameter ("multicores") (**c**, →) and occasionally affecting the same area in adjacent fibers (**d**, →) (Jungbluth, 2007).*

1.4.4 Centronuclear myopathy

Centronuclear myopathy is associated with X-linked recessive mutations in the myotubularin gene 1 (*MTM1)*, autosomal dominant mutation in dynamin 2 (*DNM2*) and amphiphysin II (*BIN1*), and autosomal recessive mutations in *RYR1*, *BIN1* and *TTN* (Jungbluth et al, 2018). Based on which gene is mutated, the disease can show different histological patterns (Figure 9). *MTM1*-related forms show central nuclei spaced along the longitudinal fiber axis, while *DNM-2*-related forms are characterized by chains of nuclei; *BIN1*-related rare forms show central nuclei forming clusters (Wilmshurst et al, 2010; Nicot et al., 2007). A typical feature of *MTM1*-related forms is the presence of central areas of increased oxidative enzyme activity with a pale peripheral halo (Ceyhan-Birsoy et al, 2010). From a clinical point of view, one of the most common features is the extraocular muscle involvement. Other common manifestations include facial weakness, external ophthalmoplegia and proximal muscle involvement.

Autosomal CNM show most frequently delayed motor milestones, distal muscle weakness, ptosis and ophthalmoplegia (Jungbluth et al, 2008).

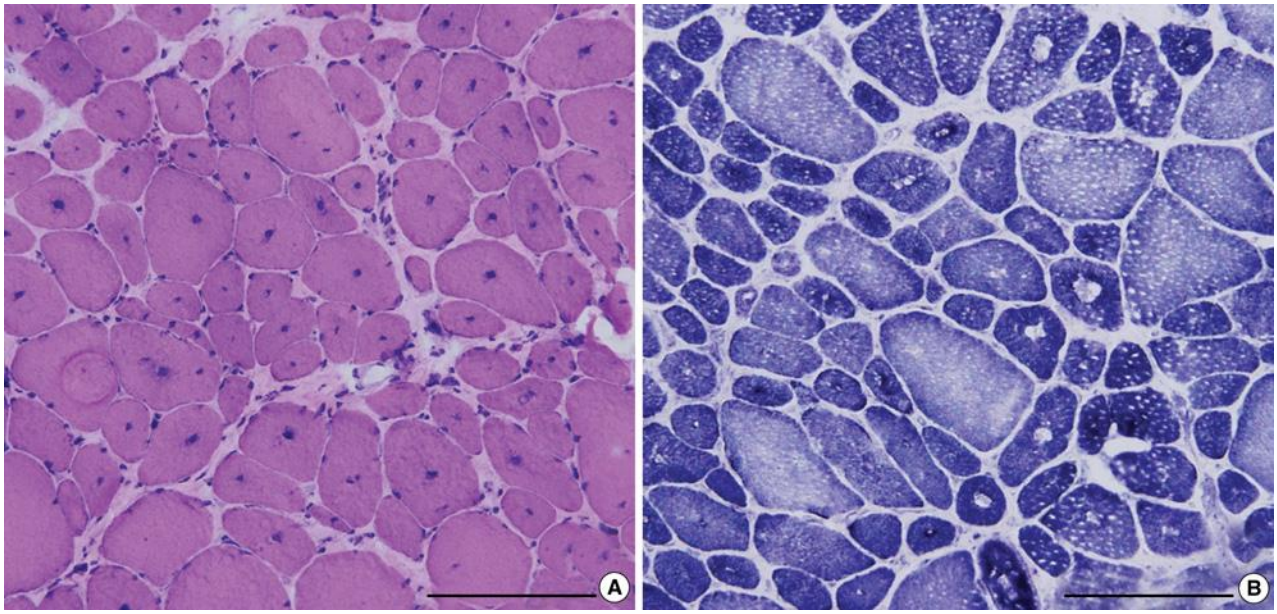

Figure 9. Centronuclear myopathy. A*. H&E staining shows centrally located nuclei in nearly all fibers with a marked variation in fiber size.* ***B.*** *NADH tetrazolium reductase staining shows type 1 fiber predominance and hypotrophy, while some fibers reveal radially arranged sarcoplasmic strands. (Lee et al, 2007)*

1.4.5 Congenital fiber type disproportion

Congenital fiber type disproportion is diagnosed by the observation of type 1 fibers size: 35-40% of them must be regularly smaller than type 2 fibers without other structural defects (Clarke et al, 2011) (Figure 10). Clinically, the disease turns up with static or slowly progressive generalized muscle weakness as well as respiratory and proximal axial weakness. Other common features are ophthalmoplegia, dysphagia and facial muscle weakness. Genetically CFTD is associated to *RYR1* variants for 20%, while other genes known to be involved are *ACTA1, TPM3, TPM2, SEPN1* and *MYH7* (Laing et al, 2004). About 30-50% of CTFD cases have not yet been associated to a genetic cause (Lawlor et al, 2010).

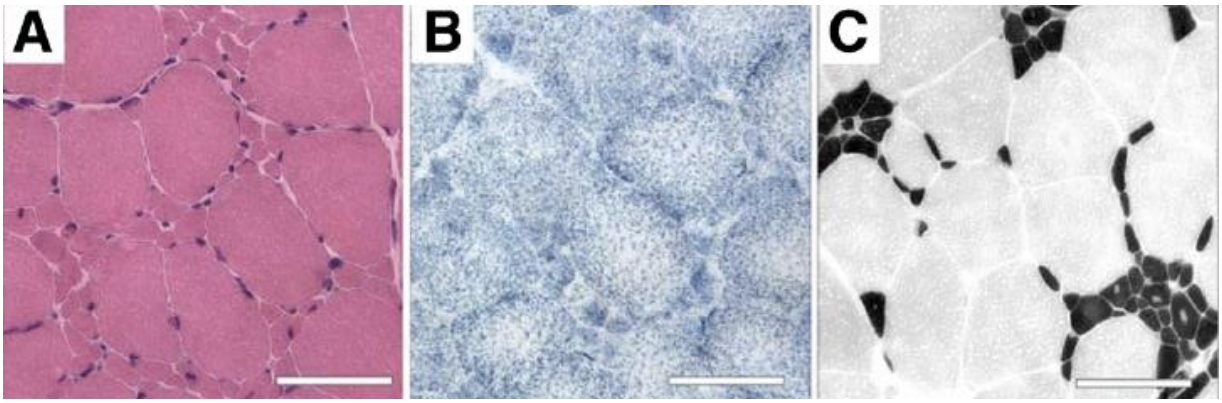

Figure 10. Histology images from patients with CFTD. *Hematoxylin and eosin (**A**) and succinate dehydrogenase (**B**) stains show normal muscle architecture except for fiber size disproportion. (**C**) ATPase (pH 4.3) stain shows type 1 fibers (dark) are consistently small, and type 2 fibers (pale) are hypertrophied. Regions of central clearing on the ATPase stain in some type 1 fibers represent internal nuclei (Clarke, 2011).*

1.4.6 Core rod myopathy

As its name suggests, muscle sections from patients with core rod myopathy (CRM) can show both central cores and nemaline bodies (rods), typical of nemaline myopathy (Figure 11). Rods are mainly composed of actin and α-actinin probably deriving from Z lines and in continuity with these structures; they can be assembled in clusters or widely distributed along the fibers (Scacheri et al, 2000). Longitudinal sections show cores with absent mitochondria covering a large part of the fibre axis. From a clinical point of view, non-specific clinical features such as hypotonia, muscle weakness, scoliosis and respiratory insufficiency are observed. The main genetic causes of CRM are *RYR1* mutations, although other causative variants have been reported (*CFL2, ACTA1, NEM1* and *TPM3*) (Lawal et al, 2018).

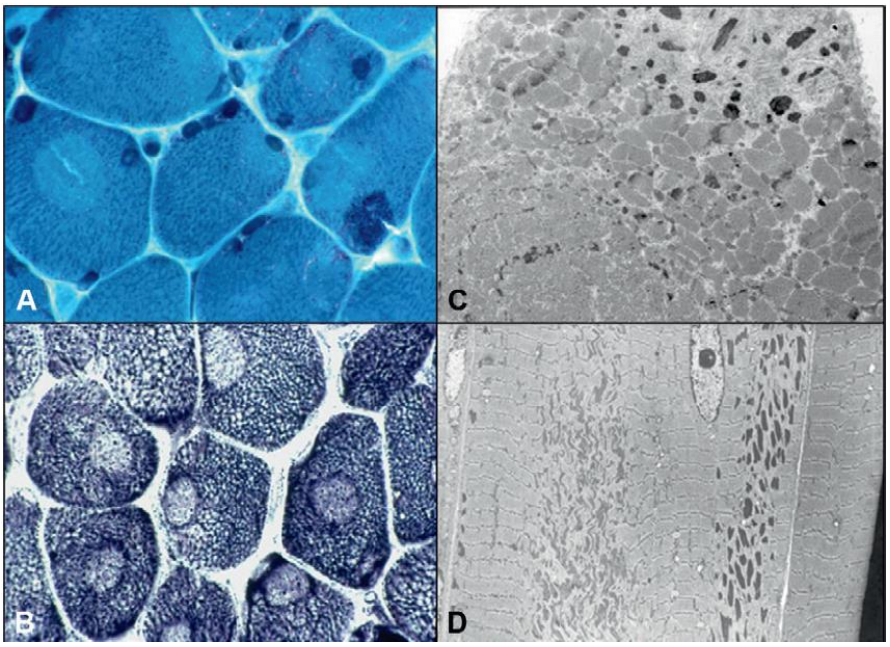

Figure 11. Core-rod myopathy. *In transverse section many muscle fibers show characteristic well-delimited cores and cluster of rods in different locations in the same fiber (**A**, Gomori trichrome (GT); **C**, NADH-TR). On electron microscopy, cores appear often in the central part of the fiber as areas of sarcomeric disorganization and reduced numbers of mitochondria; jointly, in the same fibers, numerous rods are observed in the subsarcolemmal area (**B**, transverse section; **D**, longitudinal section). (Romero and Clarke, 2013)*

1.5 Pathological mechanisms of RYR1-related myopathies

Historically, dominant *RYR1* mutations have been grouped in 3 hotspot regions, referred to as "MH/CCD hotspot": the first one, set in the N-terminal region, includes amino-acids 35-614, which span the sarcoplasmic domains; the second one, located in the central portion of the *RYR1* gene, includes amino acids 2163–2458, which also span the sarcoplasmic domain; the third, set in the C-terminal domain, corresponds to amino acids 4550–4940, which span the pore forming, the SR lumen and the transmembrane domains (Rossi and Sorrentino, 2002; Lawal et al., 2018). Generally, variants in region 1 and region 2 are predominantly associated with the MH susceptibility phenotype while those in region 3 with the CCD phenotype. Conversely, recessive inherited RYR1 variants have been reported to be distributed throughout the RYR1 sequence (Jungbluth, et al 2007). Pathological mechanisms due to RYR1 mutations can be functionally grouped into three main categories: 1) mutations causing a gain-

of-function, 2) mutations causing a loss-of-function and 3) mutations causing a reduction in RyR1 protein content.

RYR1 gain-of-function mutations can cause hypersensitivity of the channels to physiological triggers or Ca^{2+} leak. The formers are typical of MH mutations since exposure to specific triggers can lower the threshold of RyR1 activation, resulting in a massive and uncontrolled Ca^{2+} efflux from the SR (Tong et al., 1997). Generalized muscle contraction and hypermetabolic state are the main consequences of this Ca^{2+} overload, representing typical hallmarks of an MH crisis. The second kind of mutations result in spontaneous Ca^{2+} leak from the SR, that, if not counterbalanced, may cause a reduction in the SR Ca^{2+} content, leading to a diminished Ca^{2+} release upon stimulation and to reduced muscle contraction (Tong et al., 1999; Chen et al., 2017). Loss-of-function mutations result in reduction of Ca^{2+} release due to either reduced conductance caused by partial block of the channel pore (Xu et al., 2018), or impairment of RyR1 and DHPR functional coupling leading to a reduction in the amount of Ca^{2+} released following membrane depolarization, but the calcium content in the SR is normal, excluding the presence of a leaky RyR1 (Dirksen and Avila, 2002). Finally, some recessive forms of *RYR1*-related myopathies, often represented by a *RYR1* missense and a truncating mutation, cause a reduced expression of the RyR1 protein, resulting in a decrease in E-C coupling efficiency (Bevilacqua et al., 2011; Brennan et al., 2019; Monnier et al, 2008; Cacheux et al, 2015). Disease severity is linked to the nature of the mutation present in the expressed second allele as well as on the residual expression of the first-hypomorphic allele (Brennan et al., 2019; Elbaz et al., 2019).

1.6 Animal models

A comprehensive review of works published on *RYR1* variants by Lawal et al 2020, pointed out that among all *RYR1* mutations, the most frequently reported are human R614C, Y522S, I4898T and R163C. Until 1994, the R615C (corresponding to the human R614C) porcine model system has been the most frequently described. Cellular model systems to characterize RyR1 mutations have been mostly used until 2010, when there was a transition to rodent model system such as RyR1-null (dispedic) and Y524S (human Y522S), R163C (equivalent in human), and I4895T (human I4898T) mutant mice (Lawal et al, 2020).

1.6.1 Y522S mutant mice

Heterozygous expression of Y522S mutation confers susceptibility to both heat- and anesthetic-induced MH responses (Chelu et al, 2006; Michelucci et al, 2017). Homozygous Y522S knock-in mice, $RYR1^{Y522S/Y522S}$ mice, exhibit severe skeletal and muscular defects and die during embryonic development (Boncompagni et al, 2009). Functional assays on muscles from $RYR1^{Y522S/+}$ mice revealed that Ca^{2+} release channels are leaky, leading to elevation in cytosolic Ca^{2+} and a considerable reduction in SR calcium concentration; furthermore, SR calcium buffering resulted to be altered at a level comparable to that observed in calsequestrin knockout mice (Manno et al, 2013). Increase in resting Ca^{2+} is associated with ROS (reactive oxygen species), RNS (reactive nitrogen species) and basal stress production at physiologically relevant temperatures. RNS production leads to subsequent S-nitrosylation of RyR1 that further increases Ca^{2+} leak, resulting in regenerative cycle of Ca^{2+} release that underlies uncontrolled contractions during heat stress. Furthermore, uncontrolled mitochondrial superoxide production might contribute to the pathogenic temperature-dependent increase in oxidative stress of $RYR1^{Y524S/+}$ mice (Durham et al, 2008; Wei et al, 2011). Ultrastructural studies showed that mitochondrial/SR disruption may occur in confined areas, causing a significant loss of local Ca^{2+} sequestration that eventually results in the formation of contractures and progressive degradation of the contractile elements (Boncompagni et al, 2009). Therapeutic strategies to improve skeletal muscle function of mutant mice have been tested. *N*-acetylcysteine (NAC) administration turned out to be beneficial to prevent mitochondrial damage and formation of cores (Michelucci et al, 2017 II). Nevertheless, a randomized clinical trial with 63 participants showed that, after 6 months of daily administration of NAC, non-statistically significant treatment effect was observed (Todd et al, 2020).

1.6.2 R163C mutant mice

The R163C mutation in *RYR1* revealed to be responsible for DHPR activity alteration, contributing to MH episodes by altering the retrograde signal from RYR1 to the DHPR, delaying the inactivation of the DHPR voltage sensor and enhancing sarcolemmal Ca^{2+} entry during depolarization (Estève et al, 2010; Bannister et al, 2010). Developed by Yang and colleagues in 2006, the R163C heterozygous knock in mouse line immediately represented a valid animal model for studying the pathophysiology of MH, as confirmed by the observations on myotubes isolated from mice heterozygous and homozygous for the

R163C mutation that showed significantly enhanced excitation-coupled calcium entry rates, which could be restored to wild-type levels after exposure to clinical concentrations of dantrolene (Cherednichenko et al, 2008).

1.6.3 I4898T mutant mice

I4898T mutation was the first RYR1 mutation directly related to core myopathies; this kind of mutation cause a severe form of CCD in human. The first mutant mouse line carrying the I4895T mutation was generated by Zvaritch and colleagues; $RYR1^{I4895T/I4895T}$ homozygous mice were paralyzed and died perinatally. Observational and functional studies carried out on muscle, muscle sections and cultured myotubes showed a great reduction in skeletal muscle mass, with small myotubes, central nuclei and disarranged myofibrils. Nevertheless, RyR1 positioned normally at triad junctions, with the correct formation of the junctional DHPR-RyR1 macromolecular complex, but RyR1-mediated Ca^{2+} release was abolished (Zvaritch et al, 2007). Heterozygous mice show progressive formation of minicores, cores, and rods (Zvaritch et al, 2009). A deeper characterization of muscle fibers from IT/+ mice showed structural alterations similar to those observed in CCD patients (Boncompagni et al, 2010). Functional characterization of the I4898T mutation revealed that the muscle weakness observed in $RYR1^{I4895T/+}$ mice could arise from a reduction in the magnitude and rate of RYR1 Ca^{2+} release during EC coupling due to dominant-negative suppression of Ca^{2+} ion permeation (Loy et al, 2011). This mutation was actually defined as “uncoupling”, since it decreases voltage-gated Ca^{2+} release and resting cytosolic Ca^{2+} levels. In addition, involvement in voltage-induced Ca^{2+} release in hypothalamic nerve terminals was also observed in mutant mice (De Crescenzo et al. 2012). A peculiar feature of IT mice was a persistent increase in ER stress/UPR and mitochondrial ROS production that activate proapoptotic pathways and decrease protein synthesis (Malhotra et al, 2011; van Vliet et al, 2014; Lee et al, 2017). Administration of 4PBA, a chemical chaperone for restoration of protein folding demonstrated its efficacy in reducing ER stress markers, protein ubiquitination and apoptosis pathway. Furthermore, muscle function of mice treated with 4PBA improved in terms of wheel running, wire-hang performance, maximal force generation and even fiber size (Lee et al, 2017).

1.6.4 Models of recessive mutations

The generation of compound heterozygous mice in which one allele contains a frameshift deletion and the second allele a missense mutation allowed to study models of recessive RYR1-RM. In these models, a severe phenotype, that can overlap the phenotype of recessive core-like myopathies, results from a marked reduction in RyR1 protein content associated with a loss of calcium sensitivity (Brennan et al, 2019; Elbaz et al, 2019). In order to clearly assess the effects of a decreased Ryr1 expression, a mouse model characterized by a reduction in the expression of the RYR1 gene has been generated; characterization of these mice showed that RyR1 reduction is sufficient to induce a myopathic phenotype with the hallmarks of a dusty-core disease (a subgroup of Central Core Disease with exclusive RyR1 reduction) (Pelletier et al, 2020).

A mouse model mimicking recessive cases of *RYR1*-related myopathy was generated by introducing the T4706M point mutation in one allele and a 16 base pair frame-shift deletion resulting in a premature stop codon in the second allele (Brennan et al., 2019). Combination of both alleles resulted in an 80% reduction in RyR1 protein levels. The resulting mouse model presents muscle weakness, hindlimb paralysis, and severe scoliosis, but no changes in fiber type and no evidence of cores.

A second model carrying a frameshift mutation (Q1970fsX16) together with the missense mutation A4329D shows the main features of multiminicore, with a reduction in RyR1 protein level of about 65% (Elbaz et al., 2019).

1.7 ER stress and UPR

The endoplasmic reticulum (ER) is known to have many functions, among which protein folding and quality control, lipid synthesis, protein export and Ca^{2+} homeostasis (Hetz et al, 2015). The ER is involved in secretory and transmembrane protein synthesis, folding, maturation, quality control and eventually degradation. Within the ER, proteins are exposed to chaperones, foldases and post-translational modifications (Braakman et al, 2011). To cope with the possible escaping of misfolded protein, the ER has developed quality control systems to lastly correct misfolded proteins or eventually degraded it. Unrecoverable misfolded proteins are degraded by the ER-associated degradation (ERAD) process. Firstly, proteins are identified by an ER resident luminal and transmembrane protein machinery, then

retrotranslocated into the cytosol by the dislocon channel and the cytosolic AAA+ ATPase p97, deglycosylated by *N*-glycanase (NGLY1) and destined for degradation by the ubiquitin–proteasome pathway (Hebert et al, 2010; Enns et al, 2014; Huyer et al, 2004).

Conditions that perturbate the ER homeostasis can lead to the so-called ER stress. These conditions include both intrinsic and extrinsic ER elements, such as microenvironmental stress, exposure to ER stressor, reactive oxygen species production, bad modulation in temperature and others. ER stress trigger a homeostatic response, the so-called unfolded protein response (UPR), which aims at reestablishing ER homeostasis by reducing protein synthesis from one side and increasing chaperones and protein degradation from the other (Hetz, 2012).

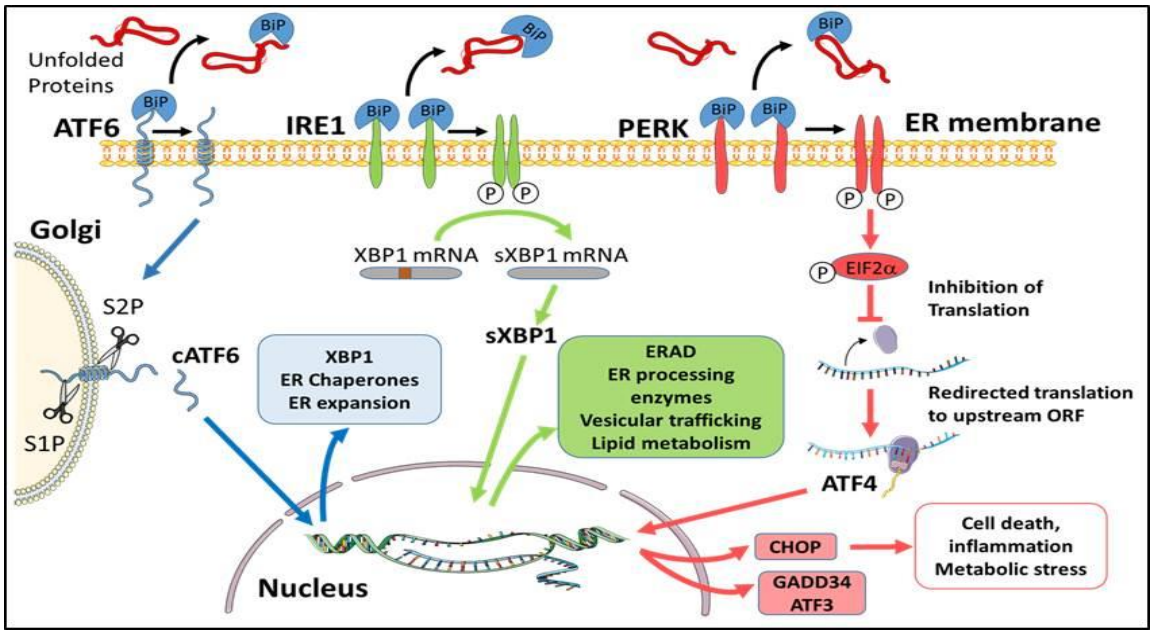

***Figure 12**. **Principal components of the UPR/ER-stress response.** ATF6, IRE1 and PERK are ER transmembrane proteins, capable of sensing the level of unfolded or misfolded proteins in the ER lumen. Upon activation, ATF6 traffics from the ER to the Golgi, where is cleaved by the site-1 and site-2 proteases freeing the N-terminal transcription factor domain (cATF6) to translocate to the nucleus and promote transcription of UPR target genes. Activation of IRE1 kinase activity is mediated by trans-autophosphorylation causing IRE1 to oligomerize in the ER membrane. Phosphorylated IRE1 excises a portion of the XBP1 mRNA forming a spliced mRNA, generating the transcription factor sXBP1. sXBP1 translocates to the nucleus and directs the expression of ER-regulators for protein folding, lipid metabolism, vesicular trafficking and acinar secretory function. Kinase activation and autophosphorylation of PERK phosphorylates the cytosolic eukaryotic translation initiation factor eIF2α thereby inhibiting global secretory protein translation. As a consequence, translation of select mRNAs including ATF4 is redirected to an upstream open reading frame giving rise to alternative protein products. ATF4 acts as a transcriptional activator or repressor, and directs the synthesis of CHOP, also a transcription factor, that plays a key role in mediating cell death, inflammation and metabolic stress. (Waldron et al, 2015)*

The aims of UPR are inhibition of protein translation to reduce overload within the ER and increasing the folding capacity of the ER in order to restore homeostasis (Sage et al, 2012). If this machinery fails, the last chance is the UPR-induced cell death. UPR is composed of three main arms initiated by, respectively, protein kinase R-like ER kinase (PERK), inositol-requiring enzyme 1-alpha (IRE1α) and activating transcription factor-6 (ATF6) (Figure 12). PERK, IRE1α and ATF6 reside on the ER membrane and are activated both by the direct contact with unfolded proteins on the luminal side and indirectly by the dissociation of chaperones such as binding immunoglobulin protein (BiP) from the receptors (Adams et al, 2019). The activation of these factors leads to downstream events that enable the resolution of ER stress.

When BiP detaches from the ER luminal domain of PERK, it oligomerizes leading to its autophosphorylation and activation (McQuiston and Diehl, 2017). PERK active form phosphorylates eIF2α, a subunit of eIF2 that regulates the first step of protein synthesis initiation; this phosphorylation leads to the inhibition of eukaryotic translation initiation factor 2B (eIF2B) activity. The final effect is a downregulation of protein synthesis, thus reducing the workload of the ER folding machinery (Rowlands et al, 1988; Harding et al, 2000). Surprisingly, some transcripts are translated more efficiently during PERK-dependent global repression of translation initiation, such as the activating transcription factor 4 (ATF4) and, consequently, the stress-responsive gene CAAT/enhancer-binding protein (C/EBP) homologous protein (CHOP)/GADD153 (Harding et al, 2000 II). ATF4 and CHOP, that is downstream to ATF4, induce genes involved in protein synthesis and the UPR; nevertheless, eIF2α also induces gene expression of growth arrest- and DNA damage-inducible protein, GADD34, that promotes dephosphorylation of eIF2α leading to recovery from translational inhibition (Ron and Walter, 2007; Novoa et al, 2001). The double effect is, on the one hand, the translational arrest induced by p-eIF2α, which reduces protein accumulation in ER lumen, and on the other hand the ATF4 activation, which leads to the expression of adaptive genes involved in amino acid transport and metabolism, protection from oxidative stress, protein homeostasis and autophagy (Quirós et al, 2017).

IRE1α has both kinase and endonuclease activity. BiP dissociation, caused by accumulating unfolded proteins, triggers IRE1α oligomerization and activation of its cytosolic kinase domain, which is necessary to activate its cytosolic RNase domain and required to recruit tumour necrosis factor receptor-associated factor 2 (TRAF2) and JNK pathway signalling (Urano et al, 2000). Through its endonuclease

activity, IRE1α promotes splicing of a 26-base intron from X-box binding protein 1 (XBP1) mRNA (Flamment et al, 2012). Spliced XBP1 (sXBP1) functions as a transcription factor to increase gene expression of some ER chaperones involved in restoring protein folding or ERAD (Tirasophon et al, 1998). IRE1α also participates with its RNase activity to the so called IRE1-dependent decay (RIDD); in this mechanism IRE1α targets and cleaves many transcripts, including its own mRNA, which are rapidly degraded by cellular exoribonucleases, in order to restore homeostasis by reducing ER accumulating proteins (Maurel et al, 2014)

After its activation in the ER and export to the Golgi, the transcription factor ATF6 is cleaved by two Golgi proteases, which induce the release of a fragment of ~ 400 amino acids corresponding to ATF6 cytosolic N-terminal portion (ATF6f). Thanks to its nuclear localization signal and DNA-binding domains, ATF6f localizes in the nucleus, where it induces UPR gene expression (Shen et al, 2002; Yamamoto et al, 2007). Furthermore, ATF6 is also able to induce the expression of both XBP1 and CHOP to improve UPR signalling (Yoshida et al, 2001).

1.7.1 ER stress and diseases

Many extracellular stimuli and fluctuations in intracellular homeostasis may disrupt protein folding in the ER. Therefore, the cell can use its ER protein-folding status as a sensor of the intracellular homeostasis. Cell injury secondary to chronic ER stress has been increasingly implicated as a central contributor to the pathophysiology of a wide range of prevalent human diseases (Wang et al, 2012). For example, prolonged ER stress and UPR signalling have been well documented in affected tissues in diabetes, neurodegenerative diseases, viral infection, inflammatory disorders, cancer, heart disease, stroke, pulmonary fibrosis. As skeletal muscle diseases are concerned, activation of ER stress-/UPR-pathway can be observed in Idiopathic inflammatory myopathies (IIM), a group of acquired myopathies characterized by chronic muscle inflammation associated with progressive muscular weakness. Among these, in the inclusion body myositis, vacuoles containing misfolded proteins can be observed, although the exact pathogenic mechanism of the disease is not completely known (Askanas and Engel, 2003). Muscular dystrophies are a phenotypically and genotypically heterogeneous group of inherited muscular disorders due to mutations in genes coding for extracellular matrix proteins, members of the dystrophin-glycoprotein complex, nuclear envelope proteins, and mitochondrial membrane proteins (Mercuri et al., 2019). ER-stress has been identified as a relevant source of muscular damage in several

muscular dystrophies; upregulation of BiP was observed in patients with Duchenne Muscular Dystrophy, in limb-girdle muscular dystrophies (LGMD) and Tibial muscular dystrophy, associated with mutations in the TTN gene. Finally in the Glycogen storage disease type II (Pompe disease), ER-stress was suggested to be a major inductor of autophagy (Mensch and Zierz, 2020).

2. Aim of this study

Ryanodine Receptor Type 1-Related Myopathies (RYR1-RM) are a group of congenital muscle diseases related and characterized by the involvement of mutations in the ryanodine receptor calcium channel. RYR1-RMs are the most common type of non-dystrophic muscle disease, which include Malignant Hyperthermia (MH), Central Core Disease, Multi Minicore Disease, Centronuclear Myopathy and Congenital fibre type disproportion. Among RYR1-RM, Central Core disease is the more frequently diagnosed, with a great need to deeply understand the pathological mechanism underlying the onset of pathological manifestations. Knock-in mice for the I4895T mutation (I4898T in humans) associated to a severe form of CCD, develop a chronic ER stress/UPR condition, which may be involved in the mechanisms leading to the pathology. The aim of this study is to verify if muscle samples from patients affected by CCD also present a condition of ER stress upregulation, as observed in the murine model.

3. Materials and methods

3.1 DNA isolation

Genomic DNA was extracted from peripheral blood leucocytes by standard procedures (Galli et al., 2006). Alternatively, DNA was isolated from skeletal muscle samples obtained from muscle biopsies of patient affected by CCD, MH and healthy individuals. For DNA isolation from tissue samples, Gentra Puregene Kit (Qiagen) has been used, following manufacturer's instructions. Samples have been inserted in a 2 ml tube with 300 µl of Cell Lysis Solution and 1,5 µl of Purgene Proteinase K. A preliminary lysis step of 30 min at 65°C in a thermostatic bath have been performed; then, samples have been kept overnight at 55°C. The day after, 100 µl of protein precipitation solution have been added and samples have been vortexed and centrifuged 3 min at 16.000 x g. Supernatant have been added to a new 1,5 ml tube with 300 µl of isopropanol; samples have been mixed by inversion 50 times and centrifuged 1 min at 16.000 x g. Supernatant has been discarded and 300 µl of 70 % ethanol have been added to the pellet. Samples have been centrifuged 1 min at 16.000 x g and the supernatant discarded again. Pellet have been allowed to air dry for 10 minutes and then resuspend with 40 µl RNAse/DNAse free water and incubated 1 hour at 65°C to dissolve the DNA. DNA obtained have been stored at 4°C until use.

3.2 Genetics

Mutation screening was performed by Next Generation Sequencing technology using the Ion GeneStudio S5 System technology (Thermo Fisher Scientific). Gene coverage for RYR1 sequence was >99%. To analyse the data obtained, a routine bioinformatic pipeline that adopts the S5 Torrent Server VM was applied (Thermo Fisher Scientific).

3.3 RNA isolation

RNA isolation has been performed by using RNeasy Mini Kit (Qiagen) following the manufacturer instructions. The whole protocol has been performed on ice. Frozen samples have been added to a 2 ml tube containing 700 µl Qiazol reagent and homogenized by using Tissue Ruptor. 140 µl of chloroform have been added and samples have been mixed by shaking; samples have been centrifuged at 15 min at 12.000 x g at 4°C. The upper aqueous phase has been transferred to a new collection tube and added

with 100% ethanol. Samples have been added to a RNeasy Mini Spin Column and centrifuged 15 sec at 12.000 x g. The flow-through has been discarded and RWT buffer has been added; samples have been centrifuged 15 sec at 12.000 x g. The flow-through has been discarded and RPE buffer has been added to the column to wash the spin column membrane. This step has been performed twice. Columns have been centrifuged in a new collection tube at full speed for 1 min. 40 µl of RNAse free water have been pipetted to the speed column membrane and samples have been centrifuged 1 min at 12.000 x g to elute RNA. Samples obtained have been quantified by using NanoDrop and stored at -20°C.

3.4 Retro transcription

RNA retro transcription into cDNA has been performed by Promega RT kit, following manufacturer instructions. 1 µg of total RNA has been added to a tube containing 1 µl of Random Primers and H_2O to a final volume of 15 µl. Samples have been incubated 5 min at 70°C and then put on ice until the second incubation. Every sample has been added with; 1X M-MLV buffer; 0,5 mM dNTPs mix; 25 U RNAsin; 200 U M-MLV Reverse Transcriptase; RNAse free H_20 to a final volume of 25 µl. Samples have been incubated 60 min at 42°C and then stored at -20°C.

3.5 Quantitative PCR (qPCR)

The expression of six genes considered to be ER stress markers has been quantified by quantitative/real time PCR on Step One Plus Real Time PCR System (Applied Biosystem). β-actin has been used as house-keeping. For each primer pair, a mix containing from 50 nM to 300 nM of Forward and Reverse primers 0.5 µl of cDNA from reverse transcription and SYBR Green PCR Fast Master Mix (Applied Biosystem) was prepared. Primers' sequence is reported in table 1. The amplification program is reported in table 2. ΔΔCT method for quantification has been used.

3.6 Statistical analysis

T-student test has been used to determine statistical significance.

Primer Forward BIP	5’ – CCGAGGAGGAGGACAAGAAG – 3’
Primer Reverse BIP	5’ – ACATAGGACGGCGTGATGC – 3’
Primer Forward β-actina	5’ – GATGAGATTGGCATGGCTTT – 3’
Primer Reverse β-actina	5’ – CACCTTCACCGTTCCAGTTT – 3’
Primer Forward CHOP	5’– CATCACCACACCTGAAAGCA – 3’
Primer Reverse CHOP	5’ –TCAGCTGCCATCTCTGCA – 3’
Primer Forward ATF4	5’–GGTTCTCCAGCGACAAGG–3’
Primer Reverse ATF4	5’– TCTCCAACATCCAATCTGTCC–3’
Primer Forward GADD34	5’–GAGGAGGCTGAAGACAGTGG –3’
Primer Reverse GADD34	5’–AATTGACTTCCCTGCCCTCT –3’
Primer Forward ERO1a	5’–TAATCCTGAGCGCTACACTGG –3’
Primer Reverse ERO1a	5’–TCACTTGTCCCTTGACCAGAA –3’
Primer Forward XBP1 spliced	5’–TGCTGAGTCCGCAGCAGGTG –3’
Primer Reverse XBP1 spliced	5’–GCTGGCAGGCTCTGGGGAAG –3’

Table 1. Sequence of the oligonucleotides used for q-PCR.

	Temperature	Time	Cycle number
Amplification	95°C	10 min	1
	95°C	3 sec	40
	60°C	30 sec	
Melting curve	95°C	15 sec	1
	60°C	1 min	1
	95°C	15 sec	1

Table 2. Amplification program used for q-PCR.

1. Results

1.1 Patients

Twenty-two unrelated patients affected by CCD and diagnosed by histological and genetic analysis (Next Generation Sequencing) were included in this study. Muscle biopsies, harvested from vastus lateralis (9), quadriceps (11) or soleus (2), were collected in a period of over 20 years (2000-2020) by 4 different Italian and Canadian hospitals. At time of biopsies collection, the age of patients was between 1 and 62 years-old, due to different age at onset: at birth or in early childhood (9), in youth (5) or in adult/late life (8). Patients presented a variety of signs and symptoms at onset: fatigue, muscle pain, iperCKemia, low back pain, mild motor impairment Achille's tendon contractures, motor delay, proximal weakness, congenital hypotonia or hypotonia, dysphagia, respiratory insufficiency, myalgia post exercise, ankle and elbow contractures. These symptoms combine into different degrees of severity: mild (14), intermediate (6) and severe (2) according to Todd et al., 2018.

1.2 Genetic analysis

Mutation screening was performed by Next Generation Sequencing technology with a gene coverage of >99% for RYR1 sequence. Overall, twenty-eight mutations have been identified; five are located into the N-terminal domain, two are located into the SPRY domains, nine into the B-Solenoid domain, three into the C-Solenoid domain and eight into the C-terminal domain. Sixteen out of twenty-four mutations are located into the three known MH/CCD hotspots of *RYR1* gene. Seven patients resulted to carry more than one mutation. The location of every single mutation into *RYR1* domains is shown in figure 13 A,B.

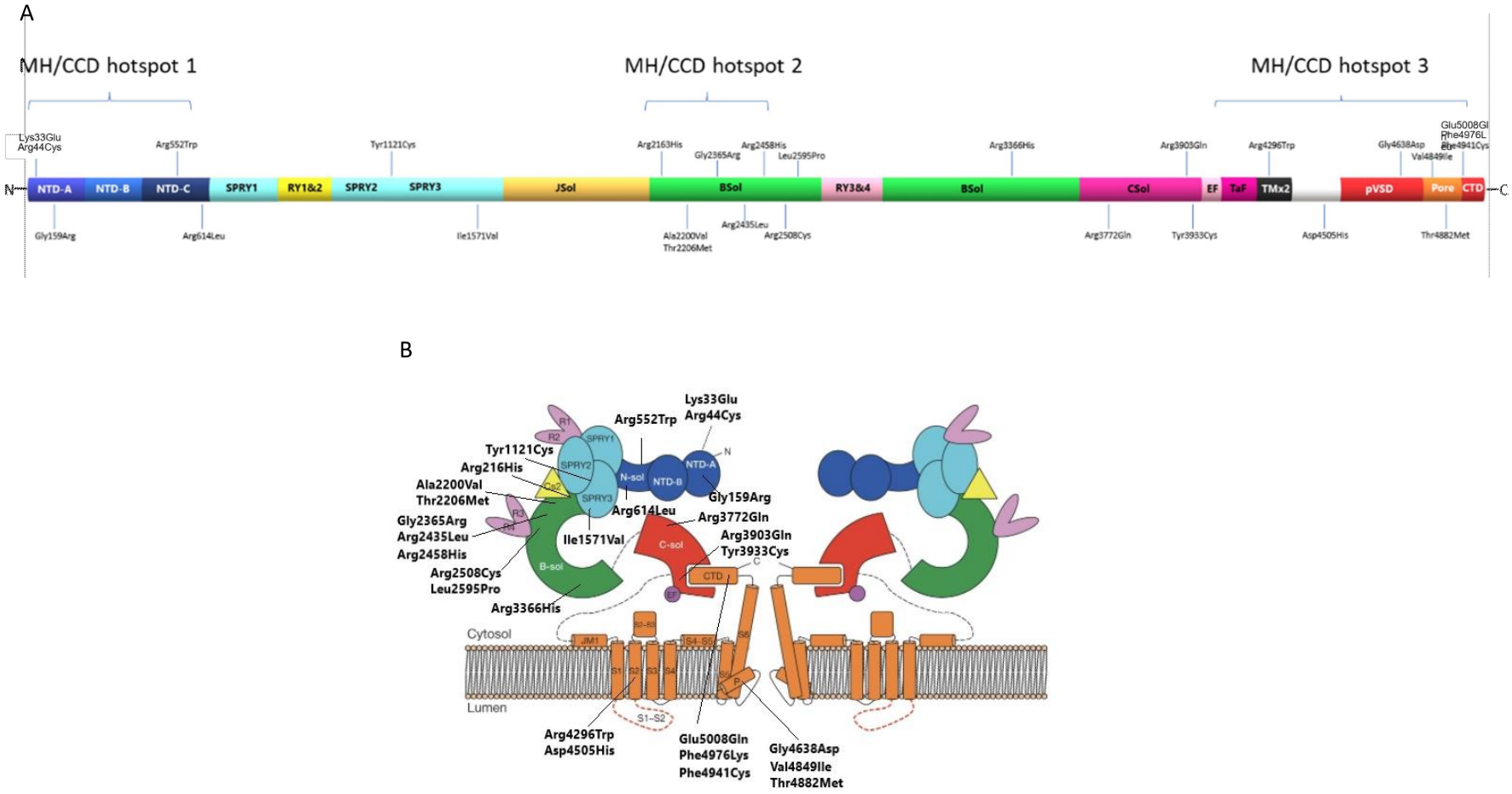

Figure 13.A. Localization of mutations on RYR1 domains; on the top, hotspot regions for MH/CCD are shown. B. Localization of mutations on a schematic representation of RyR1 structure and position (adapted from: Zalk et al, 2014; courtesy of dott. Marta Soldaini)

1.3 Mutations

Mutations obtained have been screened by using online software for predictions of the functional effect and databases of mutations that include data from literature. The software and databases used are: GnomAD (https://gnomad.broadinstitute.org/), ClinVar (https://www.ncbi.nlm.nih.gov/clinvar/) and PolyPhen-2 (http://genetics.bwh.harvard.edu/pph2/). Not every mutation has been included in all databases yet, thus for some of them only PolyPhen-2 prediction is available. It is known that susceptibility to MH is often associated to CCD; therefore, in this analysis we included the presence of the mutations in EMHG databases of diagnostic mutations for malignant hyperthermia. 8 mutations (T2206M, R2458H, V4849I, R614L, R44C, R2163H, R2508C, R552W) are included into the EMHG databases as diagnostic mutations for malignant hyperthermia. M1493V has not been described yet, as well as L2595P and E5008Q; all the other mutations have been previously reported in association with MH and or/core myopathies, according to GnomAD. 3 unrelated patients show the same three different mutations associated: two patients carry R3366H, Y3933C and I1571V, both on the same allele; another patient carries Y3933C and R3366H on the same allele. The occurrence of this triplet of RYR1 variants has been previously reported (Kraeva et al, 2015). The PolyPhen-2 score ranges from 0.0 (tolerated) to 1.0 (deleterious); variants with scores of 0.0 to 0.15 are predicted to be benign, variants with scores between 0.15 and 1.0 are classified as possibly damaging; variants with scores of 0.85 to 1.0 are more confidently predicted to be damaging, so are classified as probably damaging. PolyPhen-2 prediction of functional effect of mutations is benign for just two mutations (I1571V and R4296W); three are classified as possibly damaging (M1493V, A2200V, R3366H); all the other mutations are predicted to be probably damaging, according to PolyPhen-2 classification. Allele frequency and PolyPhen-2 scores and prediction for every mutation are reported in table 3.

ID	Age at biopsy	Mut 1st allele RYR1		Frequency	PolyPhen-2 score	Mut 2nd allele RYR1		Frequency	PolyPhen-2 score
S-AM1	54	G4638D	c.13913G>A	not reported	probably damaging, score: 1.00				
S-AM6	62	R614L	c.1841G>T	not reported	probably damaging, score: 1.00				
S-AM17	31	R44C	c.130C>T	4.13e-6	probably damaging, score: 1.00				
V-GV1	47	L2595P	c.7785C>T	not reported	probably damaging, score: 0.998				
V-GV2	20	R2163H	c.6488G>A	not reported	probably damaging, score: 1.00				
V-GV3	17	*A4410_D4416del*							
V-GV4	20	A2200V	c.6599C>T	3.89e-5	possibly damaging, score: 0.768				
		R4296W	c.12886C>T	3.64e-4	benign, score: 0.0				
VA-4636	54	T2206M	c.6617C>T	2.12e-5	probably damaging, score: 1.00				
LS-4082	53	K33E	c.97A>G	not reported	probably damaging, score: 1.00				
FIO	15	Y1121C	c.3362A>G	7.96e-6	probably damaging, score: 1.00	R3772Q	c.11315G>A	1.78e-5	probably damaging, score: 0.999
PI	3	T4882M	c.14645C>T	2.39e-5	probably damaging, score: 1.00	R3366H	c.10097G>A	8.60e-4	possibly damaging, score: 0.923
		M1493V	c.4477A>G	3.98e-6	possibly damaging, score: 0.898	Y3933C	c.11798A>G	8.49e-4	probably damaging, score: 1.00
						I1571V	c.4711A>G	8.55e-4	benign, score: 0.131
AN	2	R3903Q	c.11708G>A	1.19e-5	probably damaging, score: 1.00	F4976L	c.14928C>G	7.07e-6	probably damaging, score: 0.994
CYR	3	*F3096del*				V4849I	c.14545G>A	1.77e-5	probably damaging, score: 0.999
CI	5	S4028L	c.12083C>T	not reported	probably damaging, score: 0.970				
MU	4	Y3933C	c.11798A>G	8.49e-4	probably damaging, score: 1.00	R2458H	c.7373G>A	7.96e-6	probably damaging, score: 0.999
		R3366H	c.10097G>A	8.60e-4	possibly damaging, score: 0.923				
VA	1	D4505H	c.13513G>C	3.31e-3	probably damaging, score: 1.00				
PAP	58	R552W	c.1654C>T	3.98e-6	probably damaging, score: 0.999				
CA	22	R2435L	c.7304 G>T	not reported	probably damaging, score: 0.993				
SAN	1	E5008Q	c.15022G>C	not reported	probably damaging, score: 0.997	R3366H	c.10097G>A	8.60e-4	possibly damaging, score: 0.923
						Y3933C	c.11798A>G	8.49e-4	probably damaging, score: 1.00
						I1571V	c.4711A>G	8.55e-4	benign, score: 0.131
T1		F4941C	c.14822T>G	not reported	probably damaging, score: 0.999				
T2		G159R	c.475G>A	not reported	probably damaging, score: 1.00				
T3		R2508C	c.7522C>T	not reported	probably damaging, score: 1.00				

Table 3. Mutations of samples analyzed. For every patient is reported: identifier code, age at biopsy, mutations, frequency, when available, PolyPhen-2 prediction and scores.

1.4 ER stress evaluation on CCD samples

Data collected by Hamilton group on RYR1$^{I4895T/+}$ mice showed an increase of ER stress/UPR. In order to evaluate a possible increase of ER stress/UPR in CCD human samples carrying *RYR1* mutations, quantification by q-PCR of 6 genes considered to be ER stress/UPR markers has been performed. Our group composed of 22 samples has been compared to 25 healthy controls. The control group was selected to be as paired as possible to the affected group. Our results showed that there's not a general trend supporting ER stress/UPR increase for all the markers evaluated. GADD34 is the only gene where a significant increase in CCD samples compared to controls (p=0,02) was observed. However, this is mainly due to two biopsies (VGV3 and VGV4) which expressed about 7 fold and two patients (VGV1 and VGV2) that expressed about 3 fold higher high levels of GADD34 mRNA compared to controls. Conversely, the average levels of ATF4 (p=0,008) resulted to be significantly decreased in CCD samples compared to controls. CHOP, BiP, ERO1a and XBP1 spliced did not show a significant difference in expression levels between CCD biopsies compared to controls (Figure 14A and 14B).

A

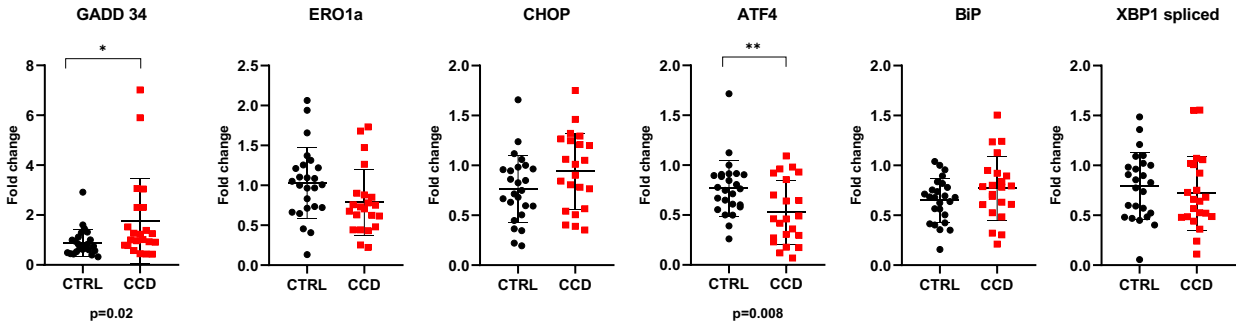

B

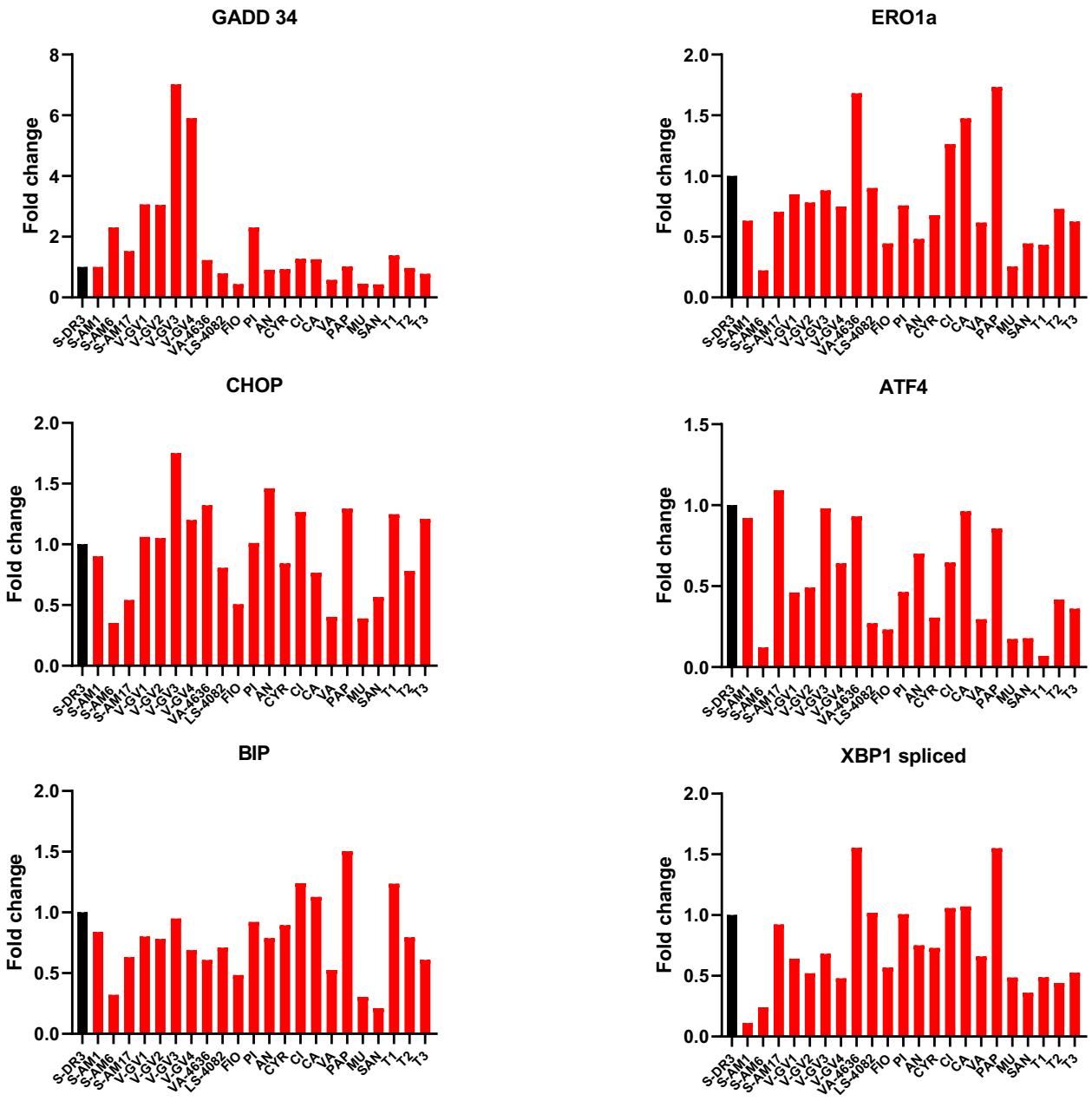

Figure 14. Results of quantitative PCR experiments on CCD samples. *ERO1, GADD34, CHOP, ATF4, BiP and XBP1 spliced have been quantified, by using β-actin as a reference gene. CCD n=22; CTRL n=25.* ***A.*** *Comparison between CCD and control groups; mean is shown for each one. ATF4 p=0,008; GADD34 p=0,02 (* p<0,05; **p<0,005; ***p<0,0005 – T-test student).* ***B.*** *Expression levels for each CCD sample compared to the reference control sample (S-DR3).*

1.5 ER stress evaluation on MH samples

To extend our analysis we evaluated the expression of ER stress/UPR markers to skeletal muscle biopsies collected from 28 patients that resulted positive for MH according to the IVCT and that carry at least one mutation in RYR1 mutation, but that do not show signs of myopathy at the histological analysis. Data obtained revealed that there is no difference in the expression levels of ER stress/UPR markers from MH samples compared to controls, with exception of XBP1 spliced, which is significantly higher in MHS samples compared to controls, with a p value of 0,003 (Figure 15).

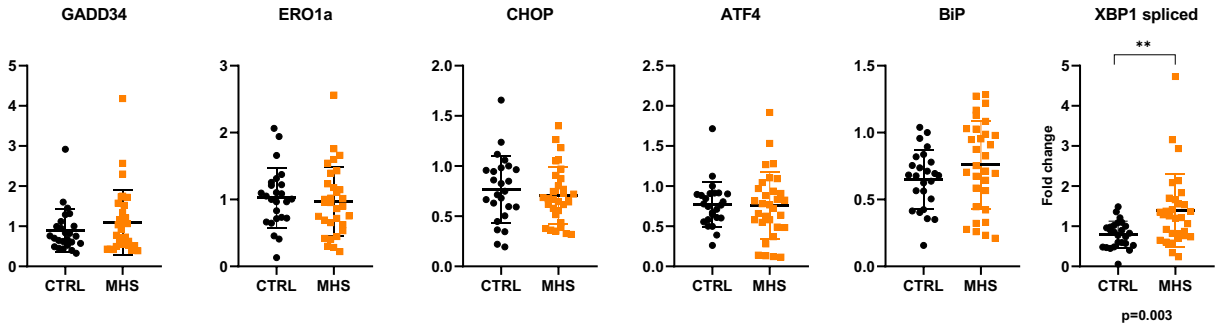

Figure 15. Results of quantitative PCR experiments on MH samples. *ERO1, GADD34, CHOP, ATF4, BiP and XBP1 spliced have been quantified, by using β-actin as a reference gene. MHS=28; CTRL= 25. XBP1 spliced p=0.003 (* p<0,05; **p<0,005; ***p<0,0005 – T-test student).*

1.6 ER stress evaluation on samples with muscular diseases unrelated to CCD

We finally quantified the same ER stress/UPR genes on a set of samples from patients with muscle diseases unrelated to CCD and that, at the genetic analysis do not show mutations in *RYR1*. A total of 22 samples were analysed including 9 samples from patients affected by Tubular Aggregates Myopathy (TAM), 13 samples from patients affected by dystrophic conditions. GADD34 and XBP1 spliced resulted to have higher expression levels in disease associated samples compared to controls, with a p-value of 0,0014 and 0,0048, respectively. ERO1a, CHOP, ATF4 and BiP were expressed at comparable levels (Figure 16).

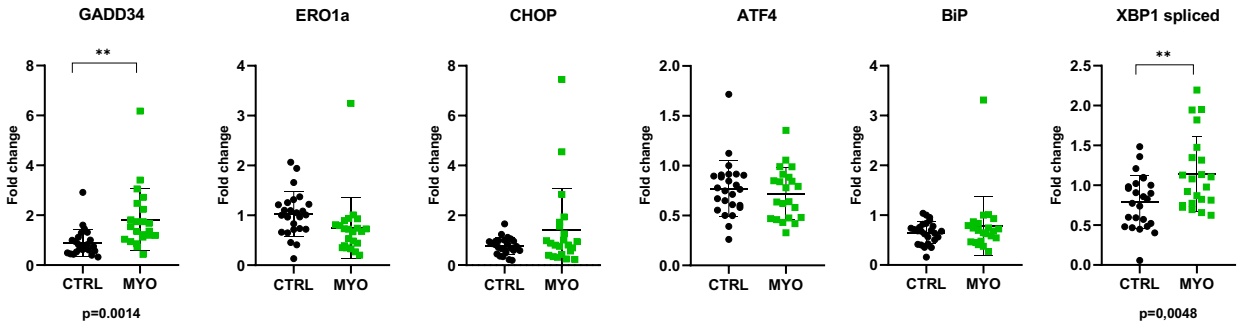

Figure 16. Results of quantitative PCR experiments on myopathic samples. *ERO1, GADD34, CHOP, ATF4, BiP and XBP1 spliced have been quantified, by using beta actin as a reference gene. MYO=22; CTRL n=25. GADD34 p=0,0014; XBP1 spliced p=0,0048 (* p<0,05; **p<0,005; ***p<0,0005 – T-test student)*

2. Discussion

Congenital myopathies are characterised by a very wide range of clinical and phenotypical manifestation. Among these myopathies, RYR1-RMs are the most frequently diagnosed (Gonorazky et al, 2018). Genotype/phenotype correlation is well documented in most of the diseases diagnosed; nevertheless, the pathological mechanisms that underlie RYR1-RMs are not fully understood and/or characterized. For this purpose, in the past decades some murine models have been generated, including a model for CCD, where mice carrying the I4895T mutation, corresponding to I4898T mutation in human, were generated and characterized (Zvaritch et al, 2007). These mice show a phenotype comparable to that observed in core-like myopathies in humans, with alterations in calcium release, delayed development and, at the histologically, the presence of minicores, cores and nemaline rods (Zvaritch et al, 2009). Studies performed on the RyR1 I4898T mouse model developed by Lee and collaborators showed that increase in ER stress/UPR in muscles may significantly contribute to muscle disease (Lee et al., 2017). This may be correlated to a decrease in triadin expression level and mislocalization of calsequestrin, that, over time, may alter the Ca^{2+} storage capacity of the SR and induce a chronic elevation of ER stress/UPR. Indeed, the I4895T mutation is close to the amino acids involved in the binding of triadin to RyR1 (Goonasekera et al, 2007) and triadin deficiency and alteration in CSQ polymerization have been found to correlated with ER stress in cardiac muscle (Cai et al, 2012; Valle et al, 2014). In particular, analysis of ER stress/UPR markers in soleus muscles from I4895T mice revealed a significant up-regulation of CHOP, BiP, ATF6 and ERO1α at all ages analysed, namely from 4 to 29 months of age; these findings suggest that all three arms of the ER stress/UPR response are persistently elevated in the muscle of IT mice. According to this hypothesis, alteration of SR Ca^{2+} handling may be translated to an increase in mitochondrial Ca^{2+} uptake. SR-mitochondrial associated membranes (SR-MaMs) in skeletal muscle are thought to play a role in handling contraction-associated energy demands with ATP production (Kaufman et al, 2014; Boncompagni et al, 2009). Although the IT mutation in RyR1 did not significantly alter the overall structures of the SR-MaMs, tethers between the SR and the mitochondria were shorter; the shorter distance between SR and mitochondria may contribute to increased mitochondrial Ca^{2+} uptake in IT muscle and ROS production (Lee et al, 2017). One of the main consequences of persistent elevations in mitochondrial Ca^{2+} and ROS production is mitochondrial damage and activation of proapoptotic pathways, such as increased caspases activity and elevation of proapoptotic protein p53. Accordingly, persistent ER stress/UPR, decrease in protein

synthesis, increase in mitochondrial Ca^{2+} uptake and ROS production, may finally end in development in core myopathy (Malhotra et al, 2011; van Vliet et al, 2014). In line to the hypothesis of ER stress/UPR, the administration of 4PBA, a molecular chaperone, was shown to reduce the expression of ER stress/UPR markers, increase protein synthesis and improve muscle function (Lee et al, 2017).

The purpose of this thesis was to verify if ER stress/UPR markers were also upregulated in human skeletal muscle biopsies from patients affected by CCD. The expression levels of 6 genes (GADD34, ERO1a, ATF4, XBP1 spliced, CHOP and BiP) have been quantified at the mRNA level. We found that, except for GADD34 that is increased in CCD compared to controls, none of the other genes resulted to be up-regulated in human CCD samples; ATF4 is decreased in CCD compared to control samples. These results indicate that, on average and at least as it concerns this sample group, no significant alterations can be observed in expression of genes coding for proteins of ER stress/UPR pathway.

Analysis of single samples shows that 22,7% (5/22) of CCD patients shows one ER stress/UPR marker that results to be upregulated compared to control; in particular, an increase in GADD34 and CHOP was observed in 3 and 2 patients, respectively. Four of these five patients carry a RYR1 mutation that is causative for MH, located in the NTD-A, B-solenoid and N-solenoid regions, with a clinic phenotype ranging from asymptomatic to mild. 18.2% (4/22) of CCD patients shows upregulation in two ER stress/UPR markers; two of them show upregulation of both CHOP and GADD34, one shows upregulation of BiP and CHOP and one shows upregulation of BiP and ERO1a. One of the two patients, patient VGV3, with upregulation of both CHOP and GADD34 carries a deletion in *RYR1* from residue 4415 to 4421, a region located upstream the pVDS domain. At clinical levels this patient shows a functional impairment of the lower limbs. The second patient (VGV4) carries two mutations, Ala2200Val (in the B-solenoid) and Arg4296Trp (located in a putative auxiliary transmembrane helix) and shows a mild clinic phenotype. Patient T1, showing upregulation of BiP and CHOP, carries mutation Phe4941Cys located in the Cytoplasmic extension of S6, and patient CA, showing upregulation of BiP and ERO1a, carries mutation Arg2435Leu in the B-solenoid. Finally, patient VA4626 showed upregulation of three ER stress/UPR genes, ERO1, CHOP and XBP1 spliced and carries mutation Thr2206Met (in B-solenoid), that is causative for MH. All patients that show an increase in at least one ER stress/UPR marker are adult patients (from 17 to 58 years of age), while the two pediatric patients analysed (1 and 3 years of age) do not show upregulation in ER stress/UPR markers. Similar to what observed in CCD patients, no

average upregulation of ER stress/UPR was observed in muscle biopsies from MH patients or in patients affected by muscle diseases not associated with RyR1 mutations.

These data indicate that at difference with what observed in the I4895T mouse model increase in ER stress/UPR upregulation does not represent a hallmark of CCD in humans at least as it concerns the RNA expression levels. Many concerns have, however, to be considered. First of all, variability in human samples is significantly higher than in the mouse model due to i) type of mutation in RyR1; ii) clinical manifestation of the disease, iii) genetic background; iv) sex and age of patients. An important point to be considered is that none of samples analysed carries the I4898Tmutation, corresponding to the murine model where ER stress elevation has been observed. We cannot thus exclude that patients carrying the I4898T mutation show a ER stress/UPR upregulation pathway similar to that observed in the mouse model. Finally, the limited size of the sample analysed does not allow to perform a robust genotype/phenotype correlation. It is important to underline that our analysis is limited to the RNA levels of ER stress/UPR markers and we cannot exclude that the protein levels of the aforementioned markers are different.

In conclusion, analysis of skeletal muscle biopsies from patients affected by CCD does not reveal an average increase in ER stress/UPR markers suggesting that this is not a hallmark of disease in humans. A further characterization of human biopsies from CCD patients may help in the identification of pathogenic mechanism leading to the disease.

3. Bibliography

Adams CJ, Kopp MC, Larburu N, Nowak PR, Ali MMU. Structure and Molecular Mechanism of ER Stress Signaling by the Unfolded Protein Response Signal Activator IRE1. Front Mol Biosci. 2019 Mar 12;6:11. doi: 10.3389/fmolb.2019.00011. PMID: 30931312; PMCID: PMC6423427.

Amador FJ, Stathopulos PB, Enomoto M, Ikura M. Ryanodine receptor calcium release channels: lessons from structure-function studies. FEBS J. 2013 Nov;280(21):5456-70. doi: 10.1111/febs.12194. Epub 2013 Mar 18. PMID: 23413940.

Amburgey K, McNamara N, Bennett LR, McCormick ME, Acsadi G, Dowling JJ. Prevalence of congenital myopathies in a representative pediatric united states population. Ann Neurol. 2011 Oct;70(4):662-5. doi: 10.1002/ana.22510. PMID: 22028225.

Askanas V, Engel WK. Proposed pathogenetic cascade of inclusion-body myositis: importance of amyloid-beta, misfolded proteins, predisposing genes, and aging. Curr Opin Rheumatol. 2003 Nov;15(6):737-44. doi: 10.1097/00002281-200311000-00009. PMID: 14569203.

Aston D, Capel RA, Ford KL, Christian HC, Mirams GR, Rog-Zielinska EA, Kohl P, Galione A, Burton RA, Terrar DA. High resolution structural evidence suggests the Sarcoplasmic Reticulum forms microdomains with Acidic Stores (lysosomes) in the heart. Sci Rep. 2017 Jan 17;7:40620. doi: 10.1038/srep40620. PMID: 28094777; PMCID: PMC5240626.

Bailey AG, Bloch EC. Malignant hyperthermia in a three-month-old American Indian infant. Anesth Analg. 1987 Oct;66(10):1043-5. PMID: 3631569.

Bannister RA, Beam KG. Ca(V)1.1: The atypical prototypical voltage-gated Ca^{2+} channel. Biochim Biophys Acta. 2013 Jul;1828(7):1587-97. doi: 10.1016/j.bbamem.2012.09.007. Epub 2012 Sep 13. PMID: 22982493; PMCID: PMC3615030.

Bannister RA, Estève E, Eltit JM, Pessah IN, Allen PD, López JR, Beam KG. A malignant hyperthermia-inducing mutation in RYR1 (R163C): consequent alterations in the functional properties of DHPR channels. J Gen Physiol. 2010 Jun;135(6):629-40. doi: 10.1085/jgp.200910329. Epub 2010 May 17. PMID: 20479108; PMCID: PMC2888063.

Barone V, Randazzo D, Del Re V, Sorrentino V, Rossi D. Organization of junctional sarcoplasmic reticulum proteins in skeletal muscle fibers. J Muscle Res Cell Motil. 2015 Dec;36(6):501-15. doi: 10.1007/s10974-015-9421-5. Epub 2015 Sep 15. PMID: 26374336.

Beard NA, Sakowska MM, Dulhunty AF, Laver DR. Calsequestrin is an inhibitor of skeletal muscle ryanodine receptor calcium release channels. Biophys J. 2002 Jan;82(1 Pt 1):310-20. doi: 10.1016/S0006-3495(02)75396-4. PMID: 11751318; PMCID: PMC1302471.

Beard NA, Wei L, Cheung SN, Kimura T, Varsányi M, Dulhunty AF. Phosphorylation of skeletal muscle calsequestrin enhances its Ca^{2+} binding capacity and promotes its association with junctin. Cell Calcium. 2008 Oct;44(4):363-73. doi: 10.1016/j.ceca.2008.01.005. PMID: 19230141.

Beard NA, Wei L, Dulhunty AF. Control of muscle ryanodine receptor calcium release channels by proteins in the sarcoplasmic reticulum lumen. Clin Exp Pharmacol Physiol. 2009 Mar;36(3):340-5. doi: 10.1111/j.1440-1681.2008.05094.x. PMID: 19278523.

Bellinger AM, Reiken S, Dura M, Murphy PW, Deng SX, Landry DW, Nieman D, Lehnart SE, Samaru M, LaCampagne A, Marks AR. Remodeling of ryanodine receptor complex causes "leaky" channels: a molecular mechanism for decreased exercise capacity. Proc Natl Acad Sci U S A. 2008 Feb 12;105(6):2198-202. doi: 10.1073/pnas.0711074105. Epub 2008 Feb 11. PMID: 18268335; PMCID: PMC2538898.

Bevilacqua JA, Monnier N, Bitoun M, Eymard B, Ferreiro A, Monges S, Lubieniecki F, Taratuto AL, Laquerrière A, Claeys KG, Marty I, Fardeau M, Guicheney P, Lunardi J, Romero NB. Recessive RYR1 mutations cause unusual congenital myopathy with prominent nuclear internalization and large areas of myofibrillar disorganization. Neuropathol Appl Neurobiol. 2011 Apr;37(3):271-84. doi: 10.1111/j.1365-2990.2010.01149.x. PMID: 21062345.

Bezprozvanny I, Watras J, Ehrlich BE. Bell-shaped calcium-response curves of Ins(1,4,5)P3- and calcium-gated channels from endoplasmic reticulum of cerebellum. Nature. 1991 Jun 27;351(6329):751-4. doi: 10.1038/351751a0. PMID: 1648178.

Boncompagni S, Rossi AE, Micaroni M, Beznoussenko GV, Polishchuk RS, Dirksen RT, Protasi F. Mitochondria are linked to calcium stores in striated muscle by developmentally regulated tethering structures. Mol Biol Cell. 2009 Feb;20(3):1058-67. doi: 10.1091/mbc.e08-07-0783. Epub 2008 Nov 26. PMID: 19037102; PMCID: PMC2633377.

Boncompagni S, Loy RE, Dirksen RT, Franzini-Armstrong C. The I4895T mutation in the type 1 ryanodine receptor induces fiber-type specific alterations in skeletal muscle that mimic premature aging. Aging Cell. 2010 Dec;9(6):958-70. doi: 10.1111/j.1474-9726.2010.00623.x. Epub 2010 Oct 21. PMID: 20961389; PMCID: PMC2980556.

Boncompagni S, Rossi AE, Micaroni M, Hamilton SL, Dirksen RT, Franzini-Armstrong C, Protasi F. Characterization and temporal development of cores in a mouse model of malignant hyperthermia. Proc Natl Acad Sci U S A. 2009 Dec 22;106(51):21996-2001. doi: 10.1073/pnas.0911496106. Epub 2009 Dec 4. PMID: 19966218; PMCID: PMC2799858.

Boncompagni S, Thomas M, Lopez JR, Allen PD, Yuan Q, Kranias EG, Franzini-Armstrong C, Perez CF. Triadin/Junctin double null mouse reveals a differential role for Triadin and Junctin in anchoring CASQ to the jSR and regulating Ca(2+) homeostasis. PLoS One. 2012;7(7):e39962. doi: 10.1371/journal.pone.0039962. Epub 2012 Jul 2. PMID: 22768324; PMCID: PMC3388061.

Boyden SE, Mahoney LJ, Kawahara G, Myers JA, Mitsuhashi S, Estrella EA, Duncan AR, Dey F, DeChene ET, Blasko-Goehringer JM, Bönnemann CG, Darras BT, Mendell JR, Lidov HG, Nishino I, Beggs AH, Kunkel LM, Kang PB. Mutations in the satellite cell gene MEGF10 cause a recessive congenital myopathy with minicores. Neurogenetics. 2012 May;13(2):115-24. doi: 10.1007/s10048-012-0315-z. Epub 2012 Feb 28. PMID: 22371254; PMCID: PMC3332380.

Braakman I, Bulleid NJ. Protein folding and modification in the mammalian endoplasmic reticulum. Annu Rev Biochem. 2011;80:71-99. doi: 10.1146/annurev-biochem-062209-093836. PMID: 21495850.

Brennan S, Garcia-Castañeda M, Michelucci A, Sabha N, Malik S, Groom L, Wei LaPierre L, Dowling JJ, Dirksen RT. Mouse model of severe recessive RYR1-related myopathy. Hum Mol Genet. 2019 Sep 15;28(18):3024-3036. doi: 10.1093/hmg/ddz105. PMID: 31107960; PMCID: PMC6737254.

Brini M, Calì T, Ottolini D, Carafoli E. The plasma membrane calcium pump in health and disease. FEBS J. 2013 Nov;280(21):5385-97. doi: 10.1111/febs.12193. Epub 2013 Mar 11. PMID: 23413890.

Bublitz M, Musgaard M, Poulsen H, Thøgersen L, Olesen C, Schiøtt B, Morth JP, Møller JV, Nissen P. Ion pathways in the sarcoplasmic reticulum Ca^{2+}-ATPase. J Biol Chem. 2013 Apr 12;288(15):10759-65. doi: 10.1074/jbc.R112.436550. Epub 2013 Feb 11. PMID: 23400778; PMCID: PMC3624456.

Bultynck G, Rossi D, Callewaert G, Missiaen L, Sorrentino V, Parys JB, De Smedt H. The conserved sites for the FK506-binding proteins in ryanodine receptors and inositol 1,4,5-trisphosphate receptors are structurally and functionally different. J Biol Chem. 2001 Dec 14;276(50):47715-24. doi: 10.1074/jbc.M106573200. Epub 2001 Oct 11. PMID: 11598113.

Cacheux M, Blum A, Sébastien M, Wozny AS, Brocard J, Mamchaoui K, Mouly V, Roux-Buisson N, Rendu J, Monnier N, Krivosic R, Allen P, Lacour A, Lunardi J, Fauré J, Marty I. Functional Characterization of a Central Core Disease RyR1 Mutation (p.Y4864H) Associated with Quantitative Defect in RyR1 Protein. J Neuromuscul Dis. 2015 Nov 20;2(4):421-432. doi: 10.3233/JND-150073. PMID: 27858745; PMCID: PMC5240544.

Cai WF, Pritchard T, Florea S, Lam CK, Han P, Zhou X, Yuan Q, Lehnart SE, Allen PD, Kranias EG. Ablation of junctin or triadin is associated with increased cardiac injury following ischaemia/reperfusion. Cardiovasc Res. 2012 May 1;94(2):333-41. doi: 10.1093/cvr/cvs119. Epub 2012 Mar 12. PMID: 22411973; PMCID: PMC3331615.

Canato M, Scorzeto M, Giacomello M, Protasi F, Reggiani C, Stienen GJ. Massive alterations of sarcoplasmic reticulum free calcium in skeletal muscle fibers lacking calsequestrin revealed by a genetically encoded probe. Proc Natl Acad Sci U S A. 2010 Dec 21;107(51):22326-31. doi: 10.1073/pnas.1009168108. Epub 2010 Dec 6. PMID: 21135222; PMCID: PMC3009789.

Chelu MG, Goonasekera SA, Durham WJ, Tang W, Lueck JD, Riehl J, Pessah IN, Zhang P, Bhattacharjee MB, Dirksen RT, Hamilton SL. Heat- and anesthesia-induced malignant hyperthermia in an RyR1 knock-in mouse. FASEB J. 2006 Feb;20(2):329-30. doi: 10.1096/fj.05-4497fje. Epub 2005 Nov 11. PMID: 16284304.

Cherednichenko G, Ward CW, Feng W, Cabrales E, Michaelson L, Samso M, López JR, Allen PD, Pessah IN. Enhanced excitation-coupled calcium entry in myotubes expressing malignant hyperthermia mutation R163C is attenuated by dantrolene. Mol Pharmacol. 2008 Apr;73(4):1203-12. doi: 10.1124/mol.107.043299. Epub 2008 Jan 2. PMID: 18171728; PMCID: PMC2735873.

Ceyhan-Birsoy O, Agrawal PB, Hidalgo C, Schmitz-Abe K, DeChene ET, Swanson LC, Soemedi R, Vasli N, Iannaccone ST, Shieh PB, Shur N, Dennison JM, Lawlor MW, Laporte J, Markianos K, Fairbrother WG, Granzier H, Beggs AH. Recessive truncating titin gene, TTN, mutations presenting as centronuclear myopathy. Neurology. 2013 Oct 1;81(14):1205-14. doi: 10.1212/WNL.0b013e3182a6ca62. Epub 2013 Aug 23. PMID: 23975875; PMCID: PMC3795603.

Clarke NF, Waddell LB, Cooper ST, Perry M, Smith RL, Kornberg AJ, Muntoni F, Lillis S, Straub V, Bushby K, Guglieri M, King MD, Farrell MA, Marty I, Lunardi J, Monnier N, North KN. Recessive mutations in RYR1 are a common cause of congenital fiber type disproportion. Hum Mutat. 2010 Jul;31(7):E1544-50. doi: 10.1002/humu.21278. PMID: 20583297.

Clarke NF. Congenital fiber-type disproportion. Semin Pediatr Neurol. 2011 Dec;18(4):264-71. doi: 10.1016/j.spen.2011.10.008. PMID: 22172422.

Copello JA, Barg S, Sonnleitner A, Porta M, Diaz-Sylvester P, Fill M, Schindler H, Fleischer S. Differential activation by Ca^{2+}, ATP and caffeine of cardiac and skeletal muscle ryanodine receptors after block by Mg2+. J Membr Biol. 2002 May 1;187(1):51-64. doi: 10.1007/s00232-001-0150-x. PMID: 12029377.

Dayal A, Schrötter K, Pan Y, Föhr K, Melzer W, Grabner M. The Ca^{2+} influx through the mammalian skeletal muscle dihydropyridine receptor is irrelevant for muscle performance. Nat Commun. 2017 Sep 7;8(1):475. doi: 10.1038/s41467-017-00629-x. PMID: 28883413; PMCID: PMC5589907.

De Crescenzo V, Fogarty KE, Lefkowitz JJ, Bellve KD, Zvaritch E, MacLennan DH, Walsh JV Jr. Type 1 ryanodine receptor knock-in mutation causing central core disease of skeletal muscle also displays a neuronal phenotype.

Proc Natl Acad Sci U S A. 2012 Jan 10;109(2):610-5. doi: 10.1073/pnas.1115111108. Epub 2011 Dec 27. PMID: 22203976; PMCID: PMC3258591.

des Georges A, Clarke OB, Zalk R, Yuan Q, Condon KJ, Grassucci RA, Hendrickson WA, Marks AR, Frank J. Structural Basis for Gating and Activation of RyR1. Cell. 2016 Sep 22;167(1):145-157.e17. doi: 10.1016/j.cell.2016.08.075. PMID: 27662087; PMCID: PMC5142848.

Dias JM, Vogel PD. Effects of small molecule modulators on ATP binding to skeletal ryanodine receptor. Protein J. 2009 Jun;28(5):240-6. doi: 10.1007/s10930-009-9189-9. PMID: 19636685.

Dirksen RT, Avila G. Altered ryanodine receptor function in central core disease: leaky or uncoupled Ca(2+) release channels? Trends Cardiovasc Med. 2002 Jul;12(5):189-97. doi: 10.1016/s1050-1738(02)00163-9. PMID: 12161072.

Dubowitz V., Sewry C.A., Oldfors A., Muscle biopsy: a practical approach (ed 5). 2020.

Ducreux S, Zorzato F, Müller C, Sewry C, Muntoni F, Quinlivan R, Restagno G, Girard T, Treves S. Effect of ryanodine receptor mutations on interleukin-6 release and intracellular calcium homeostasis in human myotubes from malignant hyperthermia-susceptible individuals and patients affected by central core disease. J Biol Chem. 2004 Oct 15;279(42):43838-46. doi: 10.1074/jbc.M403612200. Epub 2004 Aug 8. PMID: 15299003.

Durham WJ, Aracena-Parks P, Long C, Rossi AE, Goonasekera SA, Boncompagni S, Galvan DL, Gilman CP, Baker MR, Shirokova N, Protasi F, Dirksen R, Hamilton SL. RyR1 S-nitrosylation underlies environmental heat stroke and sudden death in Y522S RyR1 knockin mice. Cell. 2008 Apr 4;133(1):53-65. doi: 10.1016/j.cell.2008.02.042. PMID: 18394989; PMCID: PMC2366094.

Elbaz M, Ruiz A, Bachmann C, Eckhardt J, Pelczar P, Venturi E, Lindsay C, Wilson AD, Alhussni A, Humberstone T, Pietrangelo L, Boncompagni S, Sitsapesan R, Treves S, Zorzato F. Quantitative RyR1 reduction and loss of calcium sensitivity of RyR1Q1970fsX16+A4329D cause cores and loss of muscle strength. Hum Mol Genet. 2019 Sep 15;28(18):2987-2999. doi: 10.1093/hmg/ddz092. PMID: 31044239.

Eltit JM, Bannister RA, Moua O, Altamirano F, Hopkins PM, Pessah IN, Molinski TF, López JR, Beam KG, Allen PD. Malignant hyperthermia susceptibility arising from altered resting coupling between the skeletal muscle L-type Ca^{2+} channel and the type 1 ryanodine receptor. Proc Natl Acad Sci U S A. 2012 May 15;109(20):7923-8. doi: 10.1073/pnas.1119207109. Epub 2012 Apr 30. PMID: 22547813; PMCID: PMC3356662.

Eltit JM, Feng W, Lopez JR, Padilla IT, Pessah IN, Molinski TF, Fruen BR, Allen PD, Perez CF. Ablation of skeletal muscle triadin impairs FKBP12/RyR1 channel interactions essential for maintaining resting cytoplasmic Ca^{2+}. J Biol Chem. 2010 Dec 3;285(49):38453-62. doi: 10.1074/jbc.M110.164525. Epub 2010 Oct 6. PMID: 20926377; PMCID: PMC2992278.

Eltit JM, Li H, Ward CW, Molinski T, Pessah IN, Allen PD, Lopez JR. Orthograde dihydropyridine receptor signal regulates ryanodine receptor passive leak. Proc Natl Acad Sci U S A. 2011 Apr 26;108(17):7046-51. doi: 10.1073/pnas.1018380108. Epub 2011 Apr 11. PMID: 21482776; PMCID: PMC3084091.

Eltit JM, Yang T, Li H, Molinski TF, Pessah IN, Allen PD, Lopez JR. RyR1-mediated Ca^{2+} leak and Ca^{2+} entry determine resting intracellular Ca^{2+} in skeletal myotubes. J Biol Chem. 2010 Apr 30;285(18):13781-7. doi: 10.1074/jbc.M110.107300. Epub 2010 Mar 5. PMID: 20207743; PMCID: PMC2859541.

Endo M. Calcium-induced calcium release in skeletal muscle. Physiol Rev. 2009 Oct;89(4):1153-76. doi: 10.1152/physrev.00040.2008. PMID: 19789379.

Enns GM, Shashi V, Bainbridge M, Gambello MJ, Zahir FR, Bast T, Crimian R, Schoch K, Platt J, Cox R, Bernstein JA, Scavina M, Walter RS, Bibb A, Jones M, Hegde M, Graham BH, Need AC, Oviedo A, Schaaf CP, Boyle S, Butte AJ, Chen R, Chen R, Clark MJ, Haraksingh R; FORGE Canada Consortium, Cowan TM, He P, Langlois S, Zoghbi HY, Snyder M, Gibbs RA, Freeze HH, Goldstein DB. Mutations in NGLY1 cause an inherited disorder of the endoplasmic reticulum-associated degradation pathway. Genet Med. 2014 Oct;16(10):751-8. doi: 10.1038/gim.2014.22. Epub 2014 Mar 20. Erratum in: Genet Med. 2014 Jul;16(7):568. Chen, Rui [added]. PMID: 24651605; PMCID: PMC4243708.

Estève E, Eltit JM, Bannister RA, Liu K, Pessah IN, Beam KG, Allen PD, López JR. A malignant hyperthermia-inducing mutation in RYR1 (R163C): alterations in Ca^{2+} entry, release, and retrograde signaling to the DHPR. J Gen Physiol. 2010 Jun;135(6):619-28. doi: 10.1085/jgp.200910328. Epub 2010 May 17. PMID: 20479110; PMCID: PMC2888056.

Hopkins PM, Rüffert H, Snoeck MM, Girard T, Glahn KP, Ellis FR, Müller CR, Urwyler A; European Malignant Hyperthermia Group. European Malignant Hyperthermia Group guidelines for investigation of malignant hyperthermia susceptibility. Br J Anaesth. 2015 Oct;115(4):531-9. doi: 10.1093/bja/aev225. Epub 2015 Jul 18. PMID: 26188342.

Flamment M, Hajduch E, Ferré P, Foufelle F. New insights into ER stress-induced insulin resistance. Trends Endocrinol Metab. 2012 Aug;23(8):381-90. doi: 10.1016/j.tem.2012.06.003. Epub 2012 Jul 4. PMID: 22770719.

Franzini-Armstrong C. STUDIES OF THE TRIAD : I. Structure of the Junction in Frog Twitch Fibers. J Cell Biol. 1970 Nov 1;47(2):488-99. doi: 10.1083/jcb.47.2.488. PMID: 19866746; PMCID: PMC2108094.

Frontera WR, Ochala J. Skeletal muscle: a brief review of structure and function. Calcif Tissue Int. 2015 Mar;96(3):183-95. doi: 10.1007/s00223-014-9915-y. Epub 2014 Oct 8. PMID: 25294644.

Gehlert S, Bloch W, Suhr F. Ca^{2+}-dependent regulations and signaling in skeletal muscle: from electro-mechanical coupling to adaptation. Int J Mol Sci. 2015 Jan 5;16(1):1066-95. doi: 10.3390/ijms16011066. PMID: 25569087; PMCID: PMC4307291.

Gergs U, Berndt T, Buskase J, Jones LR, Kirchhefer U, Müller FU, Schlüter KD, Schmitz W, Neumann J. On the role of junctin in cardiac Ca^{2+} handling, contractility, and heart failure. Am J Physiol Heart Circ Physiol. 2007 Jul;293(1):H728-34. doi: 10.1152/ajpheart.01187.2006. Epub 2007 Mar 30. PMID: 17400717.

Gonorazky HD, Bönnemann CG, Dowling JJ. The genetics of congenital myopathies. Handb Clin Neurol. 2018;148:549-564. doi: 10.1016/B978-0-444-64076-5.00036-3. PMID: 29478600.

Goonasekera SA, Beard NA, Groom L, Kimura T, Lyfenko AD, Rosenfeld A, Marty I, Dulhunty AF, Dirksen RT. Triadin binding to the C-terminal luminal loop of the ryanodine receptor is important for skeletal muscle excitation contraction coupling. J Gen Physiol. 2007 Oct;130(4):365-78. doi: 10.1085/jgp.200709790. Epub 2007 Sep 10. PMID: 17846166; PMCID: PMC2151650.

Greising SM, Gransee HM, Mantilla CB, Sieck GC. Systems biology of skeletal muscle: fiber type as an organizing principle. Wiley Interdiscip Rev Syst Biol Med. 2012 Sep-Oct;4(5):457-73. doi: 10.1002/wsbm.1184. Epub 2012 Jul 18. PMID: 22811254; PMCID: PMC3874884.

Groh S, Marty I, Ottolia M, Prestipino G, Chapel A, Villaz M, Ronjat M. Functional interaction of the cytoplasmic domain of triadin with the skeletal ryanodine receptor. J Biol Chem. 1999 Apr 30;274(18):12278-83. doi: 10.1074/jbc.274.18.12278. PMID: 10212196.

Harding HP, Novoa I, Zhang Y, Zeng H, Wek R, Schapira M, Ron D. Regulated translation initiation controls stress-induced gene expression in mammalian cells. Mol Cell. 2000 Nov;6(5):1099-108. doi: 10.1016/s1097-2765(00)00108-8. PMID: 11106749.

Harding HP, Zhang Y, Bertolotti A, Zeng H, Ron D. Perk is essential for translational regulation and cell survival during the unfolded protein response. Mol Cell. 2000 May;5(5):897-904. doi: 10.1016/s1097-2765(00)80330-5. PMID: 10882126.

Hebert DN, Bernasconi R, Molinari M. ERAD substrates: which way out? Semin Cell Dev Biol. 2010 Jul;21(5):526-32. doi: 10.1016/j.semcdb.2009.12.007. Epub 2009 Dec 22. PMID: 20026414.

Hetz C. The unfolded protein response: controlling cell fate decisions under ER stress and beyond. Nat Rev Mol Cell Biol. 2012 Jan 18;13(2):89-102. doi: 10.1038/nrm3270. PMID: 22251901.

Hetz C, Chevet E, Oakes SA. Proteostasis control by the unfolded protein response. Nat Cell Biol. 2015 Jul;17(7):829-38. doi: 10.1038/ncb3184. Erratum in: Nat Cell Biol. 2015 Aug;17(8):1088. PMID: 26123108; PMCID: PMC5546321.

Horstick EJ, Linsley JW, Dowling JJ, Hauser MA, McDonald KK, Ashley-Koch A, Saint-Amant L, Satish A, Cui WW, Zhou W, Sprague SM, Stamm DS, Powell CM, Speer MC, Franzini-Armstrong C, Hirata H, Kuwada JY. Stac3 is a component of the excitation-contraction coupling machinery and mutated in Native American myopathy. Nat Commun. 2013;4:1952. doi: 10.1038/ncomms2952. PMID: 23736855; PMCID: PMC4056023.

Hu H, Wang Z, Wei R, Fan G, Wang Q, Zhang K, Yin CC. The molecular architecture of dihydropyrindine receptor/L-type Ca^{2+} channel complex. Sci Rep. 2015 Feb 10;5:8370. doi: 10.1038/srep08370. PMID: 25667046; PMCID: PMC4322351.

Huang X, Fruen B, Farrington DT, Wagenknecht T, Liu Z. Calmodulin-binding locations on the skeletal and cardiac ryanodine receptors. J Biol Chem. 2012 Aug 31;287(36):30328-35. doi: 10.1074/jbc.M112.383109. Epub 2012 Jul 6. PMID: 22773841; PMCID: PMC3436284.

Huyer G, Longsworth GL, Mason DL, Mallampalli MP, McCaffery JM, Wright RL, Michaelis S. A striking quality control subcompartment in Saccharomyces cerevisiae: the endoplasmic reticulum-associated compartment. Mol Biol Cell. 2004 Feb;15(2):908-21. doi: 10.1091/mbc.e03-07-0546. Epub 2003 Dec 10. PMID: 14668485; PMCID: PMC329403.

Jayaraman T, Brillantes AM, Timerman AP, Fleischer S, Erdjument-Bromage H, Tempst P, Marks AR. FK506 binding protein associated with the calcium release channel (ryanodine receptor). J Biol Chem. 1992 May 15;267(14):9474-7. PMID: 1374404.

Jayasinghe ID, Launikonis BS. Three-dimensional reconstruction and analysis of the tubular system of vertebrate skeletal muscle. J Cell Sci. 2013 Sep 1;126(Pt 17):4048-58. doi: 10.1242/jcs.131565. Epub 2013 Jun 26. PMID: 23813954.

Jungbluth H, Zhou H, Hartley L, Halliger-Keller B, Messina S, Longman C, Brockington M, Robb SA, Straub V, Voit T, Swash M, Ferreiro A, Bydder G, Sewry CA, Müller C, Muntoni F. Minicore myopathy with ophthalmoplegia caused by mutations in the ryanodine receptor type 1 gene. Neurology. 2005 Dec 27;65(12):1930-5. doi: 10.1212/01.wnl.0000188870.37076.f2. PMID: 16380615.

Jungbluth H, Sewry CA, Muntoni F. Core myopathies. Semin Pediatr Neurol. 2011 Dec;18(4):239-49. doi: 10.1016/j.spen.2011.10.005. PMID: 22172419.

Jungbluth H. Multi-minicore Disease. Orphanet J Rare Dis. 2007 Jul 13;2:31. doi: 10.1186/1750-1172-2-31. PMID: 17631035; PMCID: PMC1947955.

Jungbluth H, Wallgren-Pettersson C, Laporte J. Centronuclear (myotubular) myopathy. Orphanet J Rare Dis. 2008 Sep 25;3:26. doi: 10.1186/1750-1172-3-26. PMID: 18817572; PMCID: PMC2572588.

Jungbluth H, Treves S, Zorzato F, Sarkozy A, Ochala J, Sewry C, Phadke R, Gautel M, Muntoni F. Congenital myopathies: disorders of excitation-contraction coupling and muscle contraction. Nat Rev Neurol. 2018 Mar;14(3):151-167. doi: 10.1038/nrneurol.2017.191. Epub 2018 Feb 2. PMID: 29391587.

Kaufman RJ, Malhotra JD. Calcium trafficking integrates endoplasmic reticulum function with mitochondrial bioenergetics. Biochim Biophys Acta. 2014 Oct;1843(10):2233-9. doi: 10.1016/j.bbamcr.2014.03.022. Epub 2014 Mar 30. PMID: 24690484; PMCID: PMC4285153.

Kinnear NP, Wyatt CN, Clark JH, Calcraft PJ, Fleischer S, Jeyakumar LH, Nixon GF, Evans AM. Lysosomes co-localize with ryanodine receptor subtype 3 to form a trigger zone for calcium signalling by NAADP in rat pulmonary arterial smooth muscle. Cell Calcium. 2008 Aug;44(2):190-201. doi: 10.1016/j.ceca.2007.11.003. Epub 2008 Jan 11. PMID: 18191199; PMCID: PMC3982125.

Klein A, Lillis S, Munteanu I, Scoto M, Zhou H, Quinlivan R, Straub V, Manzur AY, Roper H, Jeannet PY, Rakowicz W, Jones DH, Jensen UB, Wraige E, Trump N, Schara U, Lochmuller H, Sarkozy A, Kingston H, Norwood F, Damian M, Kirschner J, Longman C, Roberts M, Auer-Grumbach M, Hughes I, Bushby K, Sewry C, Robb S, Abbs S, Jungbluth H, Muntoni F. Clinical and genetic findings in a large cohort of patients with ryanodine receptor 1 gene-associated myopathies. Hum Mutat. 2012 Jun;33(6):981-8. doi: 10.1002/humu.22056. Epub 2012 Apr 4. Erratum in: Hum Mutat. 2012 Aug;33(8):1310. PMID: 22473935.

Kaisto T, Metsikkö K. Distribution of the endoplasmic reticulum and its relationship with the sarcoplasmic reticulum in skeletal myofibers. Exp Cell Res. 2003 Sep 10;289(1):47-57. doi: 10.1016/s0014-4827(03)00231-3. PMID: 12941603.

Kraeva N, Heytens L, Jungbluth H, Treves S, Voermans N, Kamsteeg E, Ceuterick-de Groote C, Baets J, Riazi S. Compound RYR1 heterozygosity resulting in a complex phenotype of malignant hyperthermia susceptibility and a core myopathy. Neuromuscul Disord. 2015 Jul;25(7):567-76. doi: 10.1016/j.nmd.2015.04.007. Epub 2015 Apr 27. PMID: 25958340.

Laing NG, Clarke NF, Dye DE, Liyanage K, Walker KR, Kobayashi Y, Shimakawa S, Hagiwara T, Ouvrier R, Sparrow JC, Nishino I, North KN, Nonaka I. Actin mutations are one cause of congenital fibre type disproportion. Ann Neurol. 2004 Nov;56(5):689-94. doi: 10.1002/ana.20260. PMID: 15468086.

Laver DR, Owen VJ, Junankar PR, Taske NL, Dulhunty AF, Lamb GD. Reduced inhibitory effect of Mg2+ on ryanodine receptor-Ca^{2+} release channels in malignant hyperthermia. Biophys J. 1997 Oct;73(4):1913-24. doi: 10.1016/S0006-3495(97)78222-5. PMID: 9336187; PMCID: PMC1181092.

Laver DR. Ca^{2+} stores regulate ryanodine receptor Ca^{2+} release channels via luminal and cytosolic Ca^{2+} sites. Clin Exp Pharmacol Physiol. 2007 Sep;34(9):889-96. doi: 10.1111/j.1440-1681.2007.04708.x. PMID: 17645636.

Laver DR, Lenz GK, Lamb GD. Regulation of the calcium release channel from rabbit skeletal muscle by the nucleotides ATP, AMP, IMP and adenosine. J Physiol. 2001 Dec 15;537(Pt 3):763-78. doi: 10.1111/j.1469-7793.2001.00763.x. PMID: 11744753; PMCID: PMC2279010.

Lawal TA, Todd JJ, Meilleur KG. Ryanodine Receptor 1-Related Myopathies: Diagnostic and Therapeutic Approaches. Neurotherapeutics. 2018 Oct;15(4):885-899. doi: 10.1007/s13311-018-00677-1. PMID: 30406384; PMCID: PMC6277304.

Lawal TA, Wires ES, Terry NL, Dowling JJ, Todd JJ. Preclinical model systems of ryanodine receptor 1-related myopathies and malignant hyperthermia: a comprehensive scoping review of works published 1990-2019. Orphanet J Rare Dis. 2020 May 7;15(1):113. doi: 10.1186/s13023-020-01384-x. PMID: 32381029; PMCID: PMC7204063.

Lee CS, Hanna AD, Wang H, Dagnino-Acosta A, Joshi AD, Knoblauch M, Xia Y, Georgiou DK, Xu J, Long C, Amano H, Reynolds C, Dong K, Martin JC, Lagor WR, Rodney GG, Sahin E, Sewry C, Hamilton SL. A chemical chaperone improves muscle function in mice with a RyR1 mutation. Nat Commun. 2017 Mar 24;8:14659. doi: 10.1038/ncomms14659. PMID: 28337975; PMCID: PMC5376670.

Li L, Mirza S, Richardson SJ, Gallant EM, Thekkedam C, Pace SM, Zorzato F, Liu D, Beard NA, Dulhunty AF. A new cytoplasmic interaction between junctin and ryanodine receptor Ca^{2+} release channels. J Cell Sci. 2015 Mar 1;128(5):951-63. doi: 10.1242/jcs.160689. Epub 2015 Jan 20. PMID: 25609705; PMCID: PMC4342579.

Linsley JW, Hsu IU, Groom L, Yarotskyy V, Lavorato M, Horstick EJ, Linsley D, Wang W, Franzini-Armstrong C, Dirksen RT, Kuwada JY. Congenital myopathy results from misregulation of a muscle Ca^{2+} channel by mutant Stac3. Proc Natl Acad Sci U S A. 2017 Jan 10;114(2):E228-E236. doi: 10.1073/pnas.1619238114. Epub 2016 Dec 21. PMID: 28003463; PMCID: PMC5240691.

Løseth S, Voermans NC, Torbergsen T, Lillis S, Jonsrud C, Lindal S, Kamsteeg EJ, Lammens M, Broman M, Dekomien G, Maddison P, Muntoni F, Sewry C, Radunovic A, de Visser M, Straub V, van Engelen B, Jungbluth H. A novel late-onset axial myopathy associated with mutations in the skeletal muscle ryanodine receptor (RYR1) gene. J Neurol. 2013 Jun;260(6):1504-10. doi: 10.1007/s00415-012-6817-7. Epub 2013 Jan 18. PMID: 23329375.

Loy RE, Orynbayev M, Xu L, Andronache Z, Apostol S, Zvaritch E, MacLennan DH, Meissner G, Melzer W, Dirksen RT. Muscle weakness in Ryr1I4895T/WT knock-in mice as a result of reduced ryanodine receptor Ca^{2+} ion permeation and release from the sarcoplasmic reticulum. J Gen Physiol. 2011 Jan;137(1):43-57. doi: 10.1085/jgp.201010523. Epub 2010 Dec 13. PMID: 21149547; PMCID: PMC3010056.

MacIntosh BR, Holash RJ, Renaud JM. Skeletal muscle fatigue--regulation of excitation-contraction coupling to avoid metabolic catastrophe. J Cell Sci. 2012 May 1;125(Pt 9):2105-14. doi: 10.1242/jcs.093674. Epub 2012 May 24. PMID: 22627029.

Malhotra JD, Kaufman RJ. ER stress and its functional link to mitochondria: role in cell survival and death. Cold Spring Harb Perspect Biol. 2011 Sep 1;3(9):a004424. doi: 10.1101/cshperspect.a004424. PMID: 21813400; PMCID: PMC3181038.

Manno C, Figueroa L, Royer L, Pouvreau S, Lee CS, Volpe P, Nori A, Zhou J, Meissner G, Hamilton SL, Ríos E. Altered Ca^{2+} concentration, permeability and buffering in the myofibre Ca^{2+} store of a mouse model of malignant hyperthermia. J Physiol. 2013 Sep 15;591(18):4439-57. doi: 10.1113/jphysiol.2013.259572. Epub 2013 Jun 24. PMID: 23798496; PMCID: PMC3784192.

Manno C, Figueroa LC, Gillespie D, Fitts R, Kang C, Franzini-Armstrong C, Rios E. Calsequestrin depolymerizes when calcium is depleted in the sarcoplasmic reticulum of working muscle. Proc Natl Acad Sci U S A. 2017 Jan 24;114(4):E638-E647. doi: 10.1073/pnas.1620265114. Epub 2017 Jan 9. PMID: 28069951; PMCID: PMC5278470.

Manzur AY, Sewry CA, Ziprin J, Dubowitz V, Muntoni F. A severe clinical and pathological variant of central core disease with possible autosomal recessive inheritance. Neuromuscul Disord. 1998 Oct;8(7):467-73. doi: 10.1016/s0960-8966(98)00064-9. PMID: 9829276.

Marty I, Fauré J. Excitation-Contraction Coupling Alterations in Myopathies. J Neuromuscul Dis. 2016 Nov 29;3(4):443-453. doi: 10.3233/JND-160172. PMID: 27911331; PMCID: PMC5240595.

Maurel M, Chevet E, Tavernier J, Gerlo S. Getting RIDD of RNA: IRE1 in cell fate regulation. Trends Biochem Sci. 2014 May;39(5):245-54. doi: 10.1016/j.tibs.2014.02.008. Epub 2014 Mar 20. PMID: 24657016.

McQuiston A, Diehl JA. Recent insights into PERK-dependent signaling from the stressed endoplasmic reticulum. F1000Res. 2017 Oct 27;6:1897. doi: 10.12688/f1000research.12138.1. PMID: 29152224; PMCID: PMC5664976.

Mensch A, Zierz S. Cellular Stress in the Pathogenesis of Muscular Disorders-From Cause to Consequence. Int J Mol Sci. 2020 Aug 13;21(16):5830. doi: 10.3390/ijms21165830. PMID: 32823799; PMCID: PMC7461575.

Mercuri E, Bönnemann CG, Muntoni F. Muscular dystrophies. Lancet. 2019 Nov 30;394(10213):2025-2038. doi: 10.1016/S0140-6736(19)32910-1. PMID: 31789220.

Michelucci A, De Marco A, Guarnier FA, Protasi F, Boncompagni S. Antioxidant Treatment Reduces Formation of Structural Cores and Improves Muscle Function in RYR1$^{Y522S/WT}$ Mice. Oxid Med Cell Longev. 2017;2017:6792694. doi: 10.1155/2017/6792694. Epub 2017 Sep 10. PMID: 29062463; PMCID: PMC5610828.

Michelucci A, Paolini C, Boncompagni S, Canato M, Reggiani C, Protasi F. Strenuous exercise triggers a life-threatening response in mice susceptible to malignant hyperthermia. FASEB J. 2017 Aug;31(8):3649-3662. doi: 10.1096/fj.201601292R. Epub 2017 May 2. PMID: 28465322; PMCID: PMC5503704.

Miller DM, Daly C, Aboelsaod EM, Gardner L, Hobson SJ, Riasat K, Shepherd S, Robinson RL, Bilmen JG, Gupta PK, Shaw MA, Hopkins PM. Genetic epidemiology of malignant hyperthermia in the UK. Br J Anaesth. 2018 Oct;121(4):944-952. doi: 10.1016/j.bja.2018.06.028. Epub 2018 Aug 17. PMID: 30236257; PMCID: PMC6208294.

Monesi V. 2012. *Istologia*. Piccin - 6th edition

Monnier N, Marty I, Faure J, Castiglioni C, Desnuelle C, Sacconi S, Estournet B, Ferreiro A, Romero N, Laquerriere A, Lazaro L, Martin JJ, Morava E, Rossi A, Van der Kooi A, de Visser M, Verschuuren C, Lunardi J. Null mutations causing depletion of the type 1 ryanodine receptor (RYR1) are commonly associated with recessive structural congenital myopathies with cores. Hum Mutat. 2008 May;29(5):670-8. doi: 10.1002/humu.20696. PMID: 18253926.

Mukund K, Subramaniam S. Skeletal muscle: A review of molecular structure and function, in health and disease. Wiley Interdiscip Rev Syst Biol Med. 2020 Jan;12(1):e1462. doi: 10.1002/wsbm.1462. Epub 2019 Aug 13. PMID: 31407867; PMCID: PMC6916202.

Nakai J, Dirksen RT, Nguyen HT, Pessah IN, Beam KG, Allen PD. Enhanced dihydropyridine receptor channel activity in the presence of ryanodine receptor. Nature. 1996 Mar 7;380(6569):72-5. doi: 10.1038/380072a0. PMID: 8598910.

Nakai J, Sekiguchi N, Rando TA, Allen PD, Beam KG. Two regions of the ryanodine receptor involved in coupling with L-type Ca^{2+} channels. J Biol Chem. 1998 May 29;273(22):13403-6. doi: 10.1074/jbc.273.22.13403. PMID: 9593671.

Nelson BR, Wu F, Liu Y, Anderson DM, McAnally J, Lin W, Cannon SC, Bassel-Duby R, Olson EN. Skeletal muscle-specific T-tubule protein STAC3 mediates voltage-induced Ca^{2+} release and contractility. Proc Natl Acad Sci U S

A. 2013 Jul 16;110(29):11881-6. doi: 10.1073/pnas.1310571110. Epub 2013 Jul 1. PMID: 23818578; PMCID: PMC3718085.

Nicot AS, Toussaint A, Tosch V, Kretz C, Wallgren-Pettersson C, Iwarsson E, Kingston H, Garnier JM, Biancalana V, Oldfors A, Mandel JL, Laporte J. Mutations in amphiphysin 2 (BIN1) disrupt interaction with dynamin 2 and cause autosomal recessive centronuclear myopathy. Nat Genet. 2007 Sep;39(9):1134-9. doi: 10.1038/ng2086. Epub 2007 Aug 5. PMID: 17676042.

North KN, Wang CH, Clarke N, Jungbluth H, Vainzof M, Dowling JJ, Amburgey K, Quijano-Roy S, Beggs AH, Sewry C, Laing NG, Bönnemann CG; International Standard of Care Committee for Congenital Myopathies. Approach to the diagnosis of congenital myopathies. Neuromuscul Disord. 2014 Feb;24(2):97-116. doi: 10.1016/j.nmd.2013.11.003. Epub 2013 Nov 18. PMID: 24456932; PMCID: PMC5257342.

Novoa I, Zeng H, Harding HP, Ron D. Feedback inhibition of the unfolded protein response by GADD34-mediated dephosphorylation of eIF2alpha. J Cell Biol. 2001 May 28;153(5):1011-22. doi: 10.1083/jcb.153.5.1011. PMID: 11381086; PMCID: PMC2174339.

O'Reilly FM, Robert M, Jona I, Szegedi C, Albrieux M, Geib S, De Waard M, Villaz M, Ronjat M. FKBP12 modulation of the binding of the skeletal ryanodine receptor onto the II-III loop of the dihydropyridine receptor. Biophys J. 2002 Jan;82(1 Pt 1):145-55. doi: 10.1016/S0006-3495(02)75381-2. PMID: 11751303; PMCID: PMC1302456.

Oddoux S, Brocard J, Schweitzer A, Szentesi P, Giannesini B, Brocard J, Fauré J, Pernet-Gallay K, Bendahan D, Lunardi J, Csernoch L, Marty I. Triadin deletion induces impaired skeletal muscle function. J Biol Chem. 2009 Dec 11;284(50):34918-29. doi: 10.1074/jbc.M109.022442. Epub 2009 Oct 19. PMID: 19843516; PMCID: PMC2787354.

Ogasawara M, Nishino I. A review of core myopathy: central core disease, multiminicore disease, dusty core disease, and core-rod myopathy. Neuromuscul Disord. 2021 Oct;31(10):968-977. doi: 10.1016/j.nmd.2021.08.015. Epub 2021 Sep 17. PMID: 34627702.

Ohkura M, Furukawa K, Fujimori H, Kuruma A, Kawano S, Hiraoka M, Kuniyasu A, Nakayama H, Ohizumi Y. Dual regulation of the skeletal muscle ryanodine receptor by triadin and calsequestrin. Biochemistry. 1998 Sep 15;37(37):12987-93. doi: 10.1021/bi972803d. PMID: 9737879.

Paolini C, Quarta M, Nori A, Boncompagni S, Canato M, Volpe P, Allen PD, Reggiani C, Protasi F. Reorganized stores and impaired calcium handling in skeletal muscle of mice lacking calsequestrin-1. J Physiol. 2007 Sep 1;583(Pt 2):767-84. doi: 10.1113/jphysiol.2007.138024. Epub 2007 Jul 12. PMID: 17627988; PMCID: PMC2277031.

Pelletier L, Petiot A, Brocard J, Giannesini B, Giovannini D, Sanchez C, Travard L, Chivet M, Beaufils M, Kutchukian C, Bendahan D, Metzger D, Franzini Armstrong C, Romero NB, Rendu J, Jacquemond V, Fauré J, Marty I. In vivo RyR1 reduction in muscle triggers a core-like myopathy. Acta Neuropathol Commun. 2020 Nov 11;8(1):192. doi: 10.1186/s40478-020-01068-4. PMID: 33176865; PMCID: PMC7657350.

Polster A, Nelson BR, Papadopoulos S, Olson EN, Beam KG. Stac proteins associate with the critical domain for excitation-contraction coupling in the II-III loop of $Ca_V1.1$. J Gen Physiol. 2018 Apr 2;150(4):613-624. doi: 10.1085/jgp.201711917. Epub 2018 Feb 21. PMID: 29467163; PMCID: PMC5881444.

Polster A, Perni S, Bichraoui H, Beam KG. Stac adaptor proteins regulate trafficking and function of muscle and neuronal L-type Ca^{2+} channels. Proc Natl Acad Sci U S A. 2015 Jan 13;112(2):602-6. doi: 10.1073/pnas.1423113112. Epub 2014 Dec 29. PMID: 25548159; PMCID: PMC4299259.

Qi Y, Ogunbunmi EM, Freund EA, Timerman AP, Fleischer S. FK-binding protein is associated with the ryanodine receptor of skeletal muscle in vertebrate animals. J Biol Chem. 1998 Dec 25;273(52):34813-9. doi: 10.1074/jbc.273.52.34813. PMID: 9857007.

Quirós PM, Prado MA, Zamboni N, D'Amico D, Williams RW, Finley D, Gygi SP, Auwerx J. Multi-omics analysis identifies ATF4 as a key regulator of the mitochondrial stress response in mammals. J Cell Biol. 2017 Jul 3;216(7):2027-2045. doi: 10.1083/jcb.201702058. Epub 2017 May 31. PMID: 28566324; PMCID: PMC5496626.

Reiken S, Lacampagne A, Zhou H, Kherani A, Lehnart SE, Ward C, Huang F, Gaburjakova M, Gaburjakova J, Rosemblit N, Warren MS, He KL, Yi GH, Wang J, Burkhoff D, Vassort G, Marks AR. PKA phosphorylation activates the calcium release channel (ryanodine receptor) in skeletal muscle: defective regulation in heart failure. J Cell Biol. 2003 Mar 17;160(6):919-28. doi: 10.1083/jcb.200211012. Epub 2003 Mar 10. PMID: 12629052; PMCID: PMC2173774.

Ríos E. Calcium-induced release of calcium in muscle: 50 years of work and the emerging consensus. J Gen Physiol. 2018 Apr 2;150(4):521-537. doi: 10.1085/jgp.201711959. Epub 2018 Mar 7. PMID: 29514865; PMCID: PMC5881447.

Robinson R, Carpenter D, Shaw MA, Halsall J, Hopkins P. Mutations in RYR1 in malignant hyperthermia and central core disease. Hum Mutat. 2006 Oct;27(10):977-89. doi: 10.1002/humu.20356. PMID: 16917943.

Rodney GG, Krol J, Williams B, Beckingham K, Hamilton SL. The carboxy-terminal calcium binding sites of calmodulin control calmodulin's switch from an activator to an inhibitor of RYR1. Biochemistry. 2001 Oct 16;40(41):12430-5. doi: 10.1021/bi011078a. PMID: 11591164.

Romero NB, Clarke NF. Congenital myopathies. Handb Clin Neurol. 2013;113:1321-36. doi: 10.1016/B978-0-444-59565-2.00004-6. PMID: 23622357.

Ron D, Walter P. Signal integration in the endoplasmic reticulum unfolded protein response. Nat Rev Mol Cell Biol. 2007 Jul;8(7):519-29. doi: 10.1038/nrm2199. PMID: 17565364.

Rosenberg H, Davis M, James D, Pollock N, Stowell K. Malignant hyperthermia. Orphanet J Rare Dis. 2007 Apr 24;2:21. doi: 10.1186/1750-1172-2-21. PMID: 17456235; PMCID: PMC1867813.

Rossi AE, Boncompagni S, Dirksen RT. Sarcoplasmic reticulum-mitochondrial symbiosis: bidirectional signaling in skeletal muscle. Exerc Sport Sci Rev. 2009 Jan;37(1):29-35. doi: 10.1097/JES.0b013e3181911fa4. PMID: 19098522; PMCID: PMC2740713.

Rossi D, Sorrentino V. Molecular genetics of ryanodine receptors Ca^{2+}-release channels. Cell Calcium. 2002 Nov-Dec;32(5-6):307-19. doi: 10.1016/s0143416002001987. PMID: 12543091.

Rossi D, Barone V, Giacomello E, Cusimano V, Sorrentino V. The sarcoplasmic reticulum: an organized patchwork of specialized domains. Traffic. 2008 Jul;9(7):1044-9. doi: 10.1111/j.1600-0854.2008.00717.x. Epub 2008 Feb 4. PMID: 18266914.

Rossi D, Bencini C, Maritati M, Benini F, Lorenzini S, Pierantozzi E, Scarcella AM, Paolini C, Protasi F, Sorrentino V. Distinct regions of triadin are required for targeting and retention at the junctional domain of the sarcoplasmic reticulum. Biochem J. 2014 Mar 1;458(2):407-17. doi: 10.1042/BJ20130719. PMID: 24325401.

Rossi D, Lorenzini S, Pierantozzi E, Van Petegem F, Osamwonuyi Amadsun D, Sorrentino V. Multiple regions within junctin drive its interaction with calsequestrin-1 and its localization to triads in skeletal muscle. J Cell Sci. 2022 Jan 15;135(2):jcs259185. doi: 10.1242/jcs.259185. Epub 2022 Jan 25. PMID: 34913055.

Rossi D, Pierantozzi E, Amadsun DO, Buonocore S, Rubino EM, Sorrentino V. The Sarcoplasmic Reticulum of Skeletal Muscle Cells: A Labyrinth of Membrane Contact Sites. Biomolecules. 2022 Mar 23;12(4):488. doi: 10.3390/biom12040488. PMID: 35454077; PMCID: PMC9026860.

Rowlands AG, Panniers R, Henshaw EC. The catalytic mechanism of guanine nucleotide exchange factor action and competitive inhibition by phosphorylated eukaryotic initiation factor 2. J Biol Chem. 1988 Apr 25;263(12):5526-33. PMID: 3356695.

Ruehr ML, Russell MA, Ferguson DG, Bhat M, Ma J, Damron DS, Scott JD, Bond M. Targeting of protein kinase A by muscle A kinase-anchoring protein (mAKAP) regulates phosphorylation and function of the skeletal muscle ryanodine receptor. J Biol Chem. 2003 Jul 4;278(27):24831-6. doi: 10.1074/jbc.M213279200. Epub 2003 Apr 21. PMID: 12709444.

Sage AT, Holtby-Ottenhof S, Shi Y, Damjanovic S, Sharma AM, Werstuck GH. Metabolic syndrome and acute hyperglycemia are associated with endoplasmic reticulum stress in human mononuclear cells. Obesity (Silver Spring). 2012 Apr;20(4):748-55. doi: 10.1038/oby.2011.144. Epub 2011 Jun 2. PMID: 21633399.

Saito A, Inui M, Radermacher M, Frank J, Fleischer S. Ultrastructure of the calcium release channel of sarcoplasmic reticulum. J Cell Biol. 1988 Jul;107(1):211-9. doi: 10.1083/jcb.107.1.211. PMID: 2455723; PMCID: PMC2115172.

Samsó M. 3D Structure of the Dihydropyridine Receptor of Skeletal Muscle. Eur J Transl Myol. 2015 Jan 7;25(1):4840. doi: 10.4081/ejtm.2015.4840. PMID: 26913147; PMCID: PMC4748975.

Samsó M. A guide to the 3D structure of the ryanodine receptor type 1 by cryoEM. Protein Sci. 2017 Jan;26(1):52-68. doi: 10.1002/pro.3052. Epub 2016 Oct 13. PMID: 27671094; PMCID: PMC5192967.

Sandow A. Excitation-contraction coupling in skeletal muscle. Pharmacol Rev. 1965 Sep;17(3):265-320. PMID: 5318082.

Scacheri PC, Hoffman EP, Fratkin JD, Semino-Mora C, Senchak A, Davis MR, Laing NG, Vedanarayanan V, Subramony SH. A novel ryanodine receptor gene mutation causing both cores and rods in congenital myopathy. Neurology. 2000 Dec 12;55(11):1689-96. doi: 10.1212/wnl.55.11.1689. PMID: 11113224.

Schartner V, Romero NB, Donkervoort S, Treves S, Munot P, Pierson TM, Dabaj I, Malfatti E, Zaharieva IT, Zorzato F, Abath Neto O, Brochier G, Lornage X, Eymard B, Taratuto AL, Böhm J, Gonorazky H, Ramos-Platt L, Feng L, Phadke R, Bharucha-Goebel DX, Sumner CJ, Bui MT, Lacene E, Beuvin M, Labasse C, Dondaine N, Schneider R, Thompson J, Boland A, Deleuze JF, Matthews E, Pakleza AN, Sewry CA, Biancalana V, Quijano-Roy S, Muntoni F, Fardeau M, Bönnemann CG, Laporte J. Dihydropyridine receptor (DHPR, CACNA1S) congenital myopathy. Acta Neuropathol. 2017 Apr;133(4):517-533. doi: 10.1007/s00401-016-1656-8. Epub 2016 Dec 23. PMID: 28012042.

Shen J, Chen X, Hendershot L, Prywes R. ER stress regulation of ATF6 localization by dissociation of BiP/GRP78 binding and unmasking of Golgi localization signals. Dev Cell. 2002 Jul;3(1):99-111. doi: 10.1016/s1534-5807(02)00203-4. PMID: 12110171.

Shen X, Franzini-Armstrong C, Lopez JR, Jones LR, Kobayashi YM, Wang Y, Kerrick WG, Caswell AH, Potter JD, Miller T, Allen PD, Perez CF. Triadins modulate intracellular Ca(2+) homeostasis but are not essential for excitation-contraction coupling in skeletal muscle. J Biol Chem. 2007 Dec 28;282(52):37864-74. doi: 10.1074/jbc.M705702200. Epub 2007 Nov 2. PMID: 17981799.

Shin DW, Pan Z, Kim EK, Lee JM, Bhat MB, Parness J, Kim DH, Ma J. A retrograde signal from calsequestrin for the regulation of store-operated Ca^{2+} entry in skeletal muscle. J Biol Chem. 2003 Jan 31;278(5):3286-92. doi: 10.1074/jbc.M209045200. Epub 2002 Nov 4. PMID: 12419813.

Sorrentino V, Barone V, Rossi D. Intracellular Ca(2+) release channels in evolution. Curr Opin Genet Dev. 2000 Dec;10(6):662-7. doi: 10.1016/s0959-437x(00)00139-8. PMID: 11088018.

Stowell KM. Malignant hyperthermia: a pharmacogenetic disorder. Pharmacogenomics. 2008 Nov;9(11):1657-72. doi: 10.2217/14622416.9.11.1657. PMID: 19018722.

Szegedi C, Sárközi S, Herzog A, Jóna I, Varsányi M. Calsequestrin: more than 'only' a luminal Ca^{2+} buffer inside the sarcoplasmic reticulum. Biochem J. 1999 Jan 1;337 (Pt 1)(Pt 1):19-22. PMID: 9854019; PMCID: PMC1219930.

Sztretye M, Yi J, Figueroa L, Zhou J, Royer L, Allen P, Brum G, Ríos E. Measurement of RyR permeability reveals a role of calsequestrin in termination of SR Ca(2+) release in skeletal muscle. J Gen Physiol. 2011 Aug;138(2):231-47. doi: 10.1085/jgp.201010592. PMID: 21788611; PMCID: PMC3149434.

Takamori M. Structure of the neuromuscular junction: function and cooperative mechanisms in the synapse. Ann N Y Acad Sci. 2012 Dec;1274:14-23. doi: 10.1111/j.1749-6632.2012.06784.x. PMID: 23252893.

Tanabe T, Beam KG, Adams BA, Niidome T, Numa S. Regions of the skeletal muscle dihydropyridine receptor critical for excitation-contraction coupling. Nature. 1990 Aug 9;346(6284):567-9. doi: 10.1038/346567a0. PMID: 2165570.

Terentyev D, Cala SE, Houle TD, Viatchenko-Karpinski S, Gyorke I, Terentyeva R, Williams SC, Gyorke S. Triadin overexpression stimulates excitation-contraction coupling and increases predisposition to cellular arrhythmia in cardiac myocytes. Circ Res. 2005 Apr 1;96(6):651-8. doi: 10.1161/01.RES.0000160609.98948.25. Epub 2005 Feb 24. PMID: 15731460.

Timerman AP, Jayaraman T, Wiederrecht G, Onoue H, Marks AR, Fleischer S. The ryanodine receptor from canine heart sarcoplasmic reticulum is associated with a novel FK-506 binding protein. Biochem Biophys Res Commun. 1994 Jan 28;198(2):701-6. doi: 10.1006/bbrc.1994.1101. PMID: 8297381.

Tirasophon W, Welihinda AA, Kaufman RJ. A stress response pathway from the endoplasmic reticulum to the nucleus requires a novel bifunctional protein kinase/endoribonuclease (Ire1p) in mammalian cells. Genes Dev. 1998 Jun 15;12(12):1812-24. doi: 10.1101/gad.12.12.1812. PMID: 9637683; PMCID: PMC316900.

Todd JJ, Lawal TA, Witherspoon JW, Chrismer IC, Razaqyar MS, Punjabi M, Elliott JS, Tounkara F, Kuo A, Shelton MO, Allen C, Cosgrove MM, Linton M, Michael D, Jain MS, Waite M, Drinkard B, Wakim PG, Dowling JJ, Bönnemann CG, Emile-Backer M, Meilleur KG. Randomized controlled trial of *N*-acetylcysteine therapy for *RYR1*-related myopathies. Neurology. 2020 Mar 31;94(13):e1434-e1444. doi: 10.1212/WNL.0000000000008872. Epub 2020 Jan 15. PMID: 31941795; PMCID: PMC7274912.

Todd JJ, Sagar V, Lawal TA, Allen C, Razaqyar MS, Shelton MS, Chrismer IC, Zhang X, Cosgrove MM, Kuo A, Vasavada R, Jain MS, Waite M, Rajapakse D, Witherspoon JW, Wistow G, Meilleur KG. Correlation of phenotype with genotype and protein structure in RYR1-related disorders. J Neurol. 2018 Nov;265(11):2506-2524. doi: 10.1007/s00415-018-9033-2. Epub 2018 Aug 28. PMID: 30155738; PMCID: PMC6182665.

Tong J, Oyamada H, Demaurex N, Grinstein S, McCarthy TV, MacLennan DH. Caffeine and halothane sensitivity of intracellular Ca^{2+} release is altered by 15 calcium release channel (ryanodine receptor) mutations associated with malignant hyperthermia and/or central core disease. J Biol Chem. 1997 Oct 17;272(42):26332-9. doi: 10.1074/jbc.272.42.26332. PMID: 9334205.

Tong J, McCarthy TV, MacLennan DH. Measurement of resting cytosolic Ca^{2+} concentrations and Ca^{2+} store size in HEK-293 cells transfected with malignant hyperthermia or central core disease mutant Ca^{2+} release channels. J Biol Chem. 1999 Jan 8;274(2):693-702. doi: 10.1074/jbc.274.2.693. PMID: 9873004.

Treves S, Jungbluth H, Voermans N, Muntoni F, Zorzato F. Ca^{2+} handling abnormalities in early-onset muscle diseases: Novel concepts and perspectives. Semin Cell Dev Biol. 2017 Apr;64:201-212. doi: 10.1016/j.semcdb.2016.07.017. Epub 2016 Jul 15. PMID: 27427513.

Urano F, Wang X, Bertolotti A, Zhang Y, Chung P, Harding HP, Ron D. Coupling of stress in the ER to activation of JNK protein kinases by transmembrane protein kinase IRE1. Science. 2000 Jan 28;287(5453):664-6. doi: 10.1126/science.287.5453.664. PMID: 10650002.

Valle G, Boncompagni S, Sacchetto R, Protasi F, Volpe P. Post-natal heart adaptation in a knock-in mouse model of calsequestrin 2-linked recessive catecholaminergic polymorphic ventricular tachycardia. Exp Cell Res. 2014 Feb 15;321(2):178-89. doi: 10.1016/j.yexcr.2013.12.014. Epub 2013 Dec 24. PMID: 24370574.

van Vliet AR, Verfaillie T, Agostinis P. New functions of mitochondria associated membranes in cellular signaling. Biochim Biophys Acta. 2014 Oct;1843(10):2253-62. doi: 10.1016/j.bbamcr.2014.03.009. Epub 2014 Mar 15. PMID: 24642268.

Venturi E, Galfré E, O'Brien F, Pitt SJ, Bellamy S, Sessions RB, Sitsapesan R. FKBP12.6 activates RyR1: investigating the amino acid residues critical for channel modulation. Biophys J. 2014 Feb 18;106(4):824-33. doi: 10.1016/j.bpj.2013.12.041. PMID: 24559985; PMCID: PMC3945099.

Volpe P, Villa A, Podini P, Martini A, Nori A, Panzeri MC, Meldolesi J. The endoplasmic reticulum-sarcoplasmic reticulum connection: distribution of endoplasmic reticulum markers in the sarcoplasmic reticulum of skeletal muscle fibers. Proc Natl Acad Sci U S A. 1992 Jul 1;89(13):6142-6. doi: 10.1073/pnas.89.13.6142. PMID: 1631100; PMCID: PMC402138.

Waldron, Richard T. Pandol, Stephen. Lugea, Aurelia. Groblewski, Guy. Endoplasmic Reticulum Stress and the Unfolded Protein Response in Exocrine Pancreas Physiology and Pancreatitis 2015 Pancreapedia: Exocrine Pancreas Knowledge Base

Wang S, Kaufman RJ. The impact of the unfolded protein response on human disease. J Cell Biol. 2012 Jun 25;197(7):857-67. doi: 10.1083/jcb.201110131. PMID: 22733998; PMCID: PMC3384412.

Wehner M, Rueffert H, Koenig F, Neuhaus J, Olthoff D. Increased sensitivity to 4-chloro-m-cresol and caffeine in primary myotubes from malignant hyperthermia susceptible individuals carrying the ryanodine receptor 1 Thr2206Met (C6617T) mutation. Clin Genet. 2002 Aug;62(2):135-46. doi: 10.1034/j.1399-0004.2002.620206.x. PMID: 12220451.

Wehrens XH, Lehnart SE, Reiken S, van der Nagel R, Morales R, Sun J, Cheng Z, Deng SX, de Windt LJ, Landry DW, Marks AR. Enhancing calstabin binding to ryanodine receptors improves cardiac and skeletal muscle function in heart failure. Proc Natl Acad Sci U S A. 2005 Jul 5;102(27):9607-12. doi: 10.1073/pnas.0500353102. Epub 2005 Jun 22. PMID: 15972811; PMCID: PMC1172237.

Wei L, Salahura G, Boncompagni S, Kasischke KA, Protasi F, Sheu SS, Dirksen RT. Mitochondrial superoxide flashes: metabolic biomarkers of skeletal muscle activity and disease. FASEB J. 2011 Sep;25(9):3068-78. doi: 10.1096/fj.11-187252. Epub 2011 Jun 6. PMID: 21646399; PMCID: PMC3157685.

Wei R, Wang X, Zhang Y, Mukherjee S, Zhang L, Chen Q, Huang X, Jing S, Liu C, Li S, Wang G, Xu Y, Zhu S, Williams AJ, Sun F, Yin CC. Structural insights into Ca(2+)-activated long-range allosteric channel gating of RyR1. Cell Res. 2016 Sep;26(9):977-94. doi: 10.1038/cr.2016.99. Epub 2016 Aug 30. PMID: 27573175; PMCID: PMC5034117.

Weiss RG, O'Connell KM, Flucher BE, Allen PD, Grabner M, Dirksen RT. Functional analysis of the R1086H malignant hyperthermia mutation in the DHPR reveals an unexpected influence of the III-IV loop on skeletal muscle EC coupling. Am J Physiol Cell Physiol. 2004 Oct;287(4):C1094-102. doi: 10.1152/ajpcell.00173.2004. Epub 2004 Jun 16. PMID: 15201141.

Wilmshurst JM, Lillis S, Zhou H, Pillay K, Henderson H, Kress W, Müller CR, Ndondo A, Cloke V, Cullup T, Bertini E, Boennemann C, Straub V, Quinlivan R, Dowling JJ, Al-Sarraj S, Treves S, Abbs S, Manzur AY, Sewry CA, Muntoni F, Jungbluth H. RYR1 mutations are a common cause of congenital myopathies with central nuclei. Ann Neurol. 2010 Nov;68(5):717-26. doi: 10.1002/ana.22119. PMID: 20839240.

Wu S, Ibarra MC, Malicdan MC, Murayama K, Ichihara Y, Kikuchi H, Nonaka I, Noguchi S, Hayashi YK, Nishino I. Central core disease is due to RYR1 mutations in more than 90% of patients. Brain. 2006 Jun;129(Pt 6):1470-80. doi: 10.1093/brain/awl077. Epub 2006 Apr 18. PMID: 16621918.

Wu J, Yan Z, Li Z, Yan C, Lu S, Dong M, Yan N. Structure of the voltage-gated calcium channel Cav1.1 complex. Science. 2015 Dec 18;350(6267):aad2395. doi: 10.1126/science.aad2395. PMID: 26680202.

Wu J, Yan Z, Li Z, Qian X, Lu S, Dong M, Zhou Q, Yan N. Structure of the voltage-gated calcium channel Ca(v)1.1 at 3.6 Å resolution. Nature. 2016 Sep 8;537(7619):191-196. doi: 10.1038/nature19321. Epub 2016 Aug 31. PMID: 27580036.

Xu L, Chirasani VR, Carter JS, Pasek DA, Dokholyan NV, Yamaguchi N, Meissner G. Ca^{2+}-mediated activation of the skeletal-muscle ryanodine receptor ion channel. J Biol Chem. 2018 Dec 14;293(50):19501-19509. doi: 10.1074/jbc.RA118.004453. Epub 2018 Oct 19. PMID: 30341173; PMCID: PMC6302159.

Yamamoto K, Sato T, Matsui T, Sato M, Okada T, Yoshida H, Harada A, Mori K. Transcriptional induction of mammalian ER quality control proteins is mediated by single or combined action of ATF6alpha and XBP1. Dev Cell. 2007 Sep;13(3):365-76. doi: 10.1016/j.devcel.2007.07.018. PMID: 17765680.

Yamamoto T, El-Hayek R, Ikemoto N. Postulated role of interdomain interaction within the ryanodine receptor in Ca(2+) channel regulation. J Biol Chem. 2000 Apr 21;275(16):11618-25. doi: 10.1074/jbc.275.16.11618. PMID: 10766778.

Yamamoto T, Ikemoto N. Spectroscopic monitoring of local conformational changes during the intramolecular domain-domain interaction of the ryanodine receptor. Biochemistry. 2002 Feb 5;41(5):1492-501. doi: 10.1021/bi015581z. PMID: 11814342.

Yamazawa T, Takeshima H, Shimuta M, Iino M. A region of the ryanodine receptor critical for excitation-contraction coupling in skeletal muscle. J Biol Chem. 1997 Mar 28;272(13):8161-4. doi: 10.1074/jbc.272.13.8161. PMID: 9079632.

Yan Z, Bai X, Yan C, Wu J, Li Z, Xie T, Peng W, Yin C, Li X, Scheres SHW, Shi Y, Yan N. Structure of the rabbit ryanodine receptor RyR1 at near-atomic resolution. Nature. 2015 Jan 1;517(7532):50-55. doi: 10.1038/nature14063. Epub 2014 Dec 15. PMID: 25517095; PMCID: PMC4338550.

Yang T, Riehl J, Esteve E, Matthaei KI, Goth S, Allen PD, Pessah IN, Lopez JR. Pharmacologic and functional characterization of malignant hyperthermia in the R163C RyR1 knock-in mouse. Anesthesiology. 2006 Dec;105(6):1164-75. doi: 10.1097/00000542-200612000-00016. PMID: 17122579.

Yang T, Allen PD, Pessah IN, Lopez JR. Enhanced excitation-coupled calcium entry in myotubes is associated with expression of RyR1 malignant hyperthermia mutations. J Biol Chem. 2007 Dec 28;282(52):37471-8. doi: 10.1074/jbc.M701379200. Epub 2007 Oct 16. PMID: 17942409.

Yoshida H, Matsui T, Yamamoto A, Okada T, Mori K. XBP1 mRNA is induced by ATF6 and spliced by IRE1 in response to ER stress to produce a highly active transcription factor. Cell. 2001 Dec 28;107(7):881-91. doi: 10.1016/s0092-8674(01)00611-0. PMID: 11779464.

Yuan Q, Fan GC, Dong M, Altschafl B, Diwan A, Ren X, Hahn HH, Zhao W, Waggoner JR, Jones LR, Jones WK, Bers DM, Dorn GW 2nd, Wang HS, Valdivia HH, Chu G, Kranias EG. Sarcoplasmic reticulum calcium overloading in junctin deficiency enhances cardiac contractility but increases ventricular automaticity. Circulation. 2007 Jan 23;115(3):300-9. doi: 10.1161/CIRCULATIONAHA.106.654699. Epub 2007 Jan 15. PMID: 17224479.

Zalk R, Clarke OB, des Georges A, Grassucci RA, Reiken S, Mancia F, Hendrickson WA, Frank J, Marks AR. Structure of a mammalian ryanodine receptor. Nature. 2015 Jan 1;517(7532):44-9. doi: 10.1038/nature13950. Epub 2014 Dec 1. PMID: 25470061; PMCID: PMC4300236.

Zhang H, Zhang JZ, Danila CI, Hamilton SL. A noncontiguous, intersubunit binding site for calmodulin on the skeletal muscle Ca^{2+} release channel. J Biol Chem. 2003 Mar 7;278(10):8348-55. doi: 10.1074/jbc.M209565200. Epub 2002 Dec 31. PMID: 12509414.

Zhao Y, Huang G, Wu J, Wu Q, Gao S, Yan Z, Lei J, Yan N. Molecular Basis for Ligand Modulation of a Mammalian Voltage-Gated Ca^{2+} Channel. Cell. 2019 May 30;177(6):1495-1506.e12. doi: 10.1016/j.cell.2019.04.043. PMID: 31150622.

Zhou H, Rokach O, Feng L, Munteanu I, Mamchaoui K, Wilmshurst JM, Sewry C, Manzur AY, Pillay K, Mouly V, Duchen M, Jungbluth H, Treves S, Muntoni F. RyR1 deficiency in congenital myopathies disrupts excitation-contraction coupling. Hum Mutat. 2013 Jul;34(7):986-96. doi: 10.1002/humu.22326. Epub 2013 Apr 17. PMID: 23553787.

Zima AV, Bovo E, Bers DM, Blatter LA. Ca^{2}+ spark-dependent and -independent sarcoplasmic reticulum Ca^{2}+ leak in normal and failing rabbit ventricular myocytes. J Physiol. 2010 Dec 1;588(Pt 23):4743-57. doi: 10.1113/jphysiol.2010.197913. Epub 2010 Oct 20. PMID: 20962003; PMCID: PMC3010143.

Zvaritch E, Depreux F, Kraeva N, Loy RE, Goonasekera SA, Boncompagni S, Kraev A, Gramolini AO, Dirksen RT, Franzini-Armstrong C, Seidman CE, Seidman JG, Maclennan DH. An Ryr1I4895T mutation abolishes Ca^{2+} release channel function and delays development in homozygous offspring of a mutant mouse line. Proc Natl Acad Sci U S A. 2007 Nov 20;104(47):18537-42. doi: 10.1073/pnas.0709312104. Epub 2007 Nov 14. Erratum in: Proc Natl Acad Sci U S A. 2008 Jan 15;105(12):825. Boncompagi, Simona [corrected to Boncompagni, Simona]. PMID: 18003898; PMCID: PMC2141812.

Zvaritch E, Kraeva N, Bombardier E, McCloy RA, Depreux F, Holmyard D, Kraev A, Seidman CE, Seidman JG, Tupling AR, MacLennan DH. Ca^{2+} dysregulation in Ryr1(I4895T/wt) mice causes congenital myopathy with progressive formation of minicores, cores, and nemaline rods. Proc Natl Acad Sci U S A. 2009 Dec 22;106(51):21813-8. doi: 10.1073/pnas.0912126106. Epub 2009 Dec 3. PMID: 19959667; PMCID: PMC2788482.